Biopolymers for Antitumor Implantable Drug Delivery Systems: Recent Advances and Future Outlook

Talebian, Sepehr; Foroughi, Javad; Wade, Samantha J.; Vine, Kara L.; Dolatshahi-Pirouz, Alireza; Mehrali, Mehdi; Conde, João; Wallace, Gordon G.

Published in:
Advanced Materials

Link to article, DOI:
10.1002/adma.201706665

Publication date:
2018

Document Version
Peer reviewed version

Biopolymers for Antitumor Implantable Drug Delivery Systems: Recent Advances and Future Outlook

Abstract
In spite of remarkable improvements in cancer treatments and survivorship, cancer still remains as one of the major causes of death worldwide. Although current standards of care provide encouraging results, they still cause severe systemic toxicity and also fail in preventing recurrence of the disease. In order to address these issues, biomaterial-based implantable drug delivery systems (DDSs) have emerged as promising therapeutic platforms, which allow local administration of drugs directly to the tumor site. Owing to the unique properties of biopolymers, they have been used in a variety of ways to institute biodegradable implantable DDSs that exert precise spatiotemporal control over the release of therapeutic drug. Here, the most recent advances in biopolymer-based DDSs for suppressing tumor growth and preventing tumor recurrence are reviewed. Novel emerging biopolymers as well as cutting-edge polymeric microdevices deployed as implantable antitumor DDSs are discussed. Finally, a review of a new therapeutic modality within the field, which is based on implantable biopolymeric DDSs, is given.

Disciplines
Engineering | Physical Sciences and Mathematics

Publication Details
Talebian, S., Foroughi, J., Wade, S. J., Vine, K. L., Dolatshahi-Pirouz, A., Mehrali, M., Conde, J. & Wallace, G. G. (2018). Biopolymers for Antitumor Implantable Drug Delivery Systems: Recent Advances and Future Outlook. Advanced Materials, 30 (31), 1706665-2-1706665-31.

Authors
Sepehr Talebian, Javad Foroughi, Samantha Wade, Kara L. Vine, Alireza Dolatshahi-Pirouz, Mehdi Mehrali, Joao Conde, and Gordon G. Wallace

Biopolymers for anti-tumor implantable drug delivery systems: Recent advances and future outlook

Sepehr Talebian, Javad Foroughi, Samantha J Wade, Kara L. Vine, Alireza Dolatshahi-pirouz, Mehdi Mehrali, João Conde, Gordon G. Wallace* [*]*

Mr. S. Talebian
Intelligent Polymer Research Institute, ARC Centre of Excellence for Electromaterials Science, AIIM Facility, University of Wollongong, NSW, Australia
Illawarra Health and Medical Research Institute, University of Wollongong, Wollongong, NSW 2522, Australia

Dr. J. Foroughi
Intelligent Polymer Research Institute, ARC Centre of Excellence for Electromaterials Science, AIIM Facility, University of Wollongong, NSW, Australia
Illawarra Health and Medical Research Institute, University of Wollongong, Wollongong, NSW 2522, Australia

Ms. S. J Wade
Illawarra Health and Medical Research Institute, University of Wollongong, Wollongong, NSW 2522, Australia
School of Biological Sciences, University of Wollongong, NSW Australia

Dr. K.L. Vine
Illawarra Health and Medical Research Institute, University of Wollongong, Wollongong, NSW 2522, Australia
School of Biological Sciences, Centre for Medical and Molecular Bioscience, University of Wollongong, NSW Australia

Prof. A. Dolatshahi-pirouz
Technical University of Denmark, DTU Nanotech, Center for Nanomedicine and Theranostics, Kongens Lyngby, Denmark

Dr. M. Mehrali
Technical University of Denmark, DTU Nanotech, Center for Nanomedicine and Theranostics, Kongens Lyngby, Denmark

Dr. J. Conde
Massachusetts Institute of Technology, Institute for Medical Engineering and Science, Harvard-MIT Division for Health Sciences and Technology, Cambridge 02139, Massachusetts, USA

Prof. G. Wallace
Intelligent Polymer Research Institute, ARC Centre of Excellence for Electromaterials Science, AIIM Facility, University of Wollongong, NSW, Australia

Correspondence should be addressed to Dr. J. Foroughi: foroughi@uow.edu.au and Prof. G. Wallace: gwallace@uow.edu.au .

Keywords: Cancer, Drug delivery, biopolymers, casting, electrospinning, 3D printing, injectable gels, micro-device, immunotherapy

Abstract

In spite of remarkable improvements in cancer treatments and survivorship, cancer still remains as one of the major causes of death worldwide. Although current standards of care provide encouraging results, they still cause severe systemic toxicity and also fail in preventing recurrence of the disease. In order to address these issues, biomaterial-based implantable drug delivery systems (DDSs) have emerged as promising therapeutic platforms, which allow local administration of drugs directly to the tumor site. Owing to the unique properties of biopolymers, they have been used in a variety of ways to institute biodegradable implantable DDSs that exert precise spatiotemporal control over the release of therapeutic drug. Here, we review the most recent advances in biopolymer-based DDSs for suppressing tumor growth and preventing tumor recurrence. We discuss novel emerging biopolymers as well as cutting-edge polymeric micro-devices deployed as implantable anti-tumor DDSs. Lastly, a review of a new therapeutic modality within the field, which is based on implantable biopolymeric DDSs, is given.

1. Introduction

Cancer is a disease that arises from mutated cells that have acquired the capacity to proliferate indefinitely and evade apoptosis which eventually leads to tumor formation and subsequent invasion to surrounding tissues (also known as metastasis).[1, 2] Accordingly, advanced cancer is viewed as a "systemic" disease that requires systemic treatment and on account of such notion systemic administration (administered by intravenous injections) of chemotherapeutic drugs has been established as one of the standard methods to treat cancer. [3-5] Traditional systemic chemotherapy has many limitations in treating the disease including: low efficiency of delivering the drugs specifically to the tumor site at therapeutic concentrations, and the ensuing toxicity to healthy tissues. [6-8] Consequently, local delivery systems have entered the fray to address the shortcomings of systemic delivery, by delivering the drug directly to the tumor site using an implantable system (**Figure 1**). [9, 10] The implantable drug delivery system (DDS) contains one or more therapeutic agents while being placed around or inside the tumor to facilitate targeted delivery.[11, 12] These DDSs are intended to enhance drug uptake and efficacy since they (*I*) are delivered locally (directly at the site of the tumor) and therefore offer strategic and precise spatial control that significantly reduces the required drug dosage and often the side/off-target effects, (*II*) present temporal control over release profile of chemotherapeutic agents to maintain therapeutic concentrations over a longer duration of time

and (*III*) protect the loaded drugs from degradation or clearance until they are released.[4, 6, 13, 14] In the past decade, a wide variety of biomaterials have been exploited to institute anti-cancer implantable DDSs, and the properties afforded by biopolymers (such as biocompatibility, biodegradability, and ease of processing), has led to recent increased attention.[9, 15-17] A significant advantage of biopolymeric implantable DDSs is that they do not demand surgical extraction after use, as they can be cleared naturally by the body.[18]

Biopolymeric implantable DDSs are classified under two distinct categories, pre-formed systems or systems that are formed after the injection into the tumor site.[19] Pre-formed implants have been made from commercially available and FDA (U.S. Food and Drug Administration) approved synthetic biopolymers such as polycaprolactone (PCL), polylactic acid (PLA) and poly(lactic-co-glycolic) (PLGA) - or naturally occurring polymers including alginate, gelatin, silk and dextran. Pre-formed systems were typically fabricated through well-established fabrication methods such as casting, electrospinning and 3D printing.[20-39] On the other hand, in-situ formed implants are realized by direct injection into the tumor site, typically using gels that solidify in response to either temperature or pH (**Figure 1**).[40-55] Biopolymeric implantable DDSs have shown to be capable of releasing the therapeutic agents either actively (stimuli-responsive systems) or passively (non-stimuli responsive systems). Accordingly, stimuli-responsive systems showed a rapid change in dimension or physical properties, instigated by either internal stimuli within the body, such as temperature or pH, or external stimuli such as electromagnetic waves, ultrasound, visible-, infrared (IR)- and near infrared (NIR)-light (**Figure 2**).[56-60] With non-stimuli responsive systems release is passive and controlled by diffusion, drug-carrier affinity, degradation of polymer, and/or any combination of these [13, 61, 62]. Therefore, in these systems factors such as tortuosity of pores, steric interactions between drug and matrix, reversible chemical interaction of drug and matrix, and molecular weight of polymeric matrix determine the release profile of the therapeutic agent in question.[13, 63] Overall, application of the biopolymeric implantable DDSs for cancer therapy goes beyond delivery of anti-neoplastic agents (e.g. chemotherapeutic drugs), as recently they have been successfully applied to other cancer therapeutic modalities (**Figure 1**) including hyperthermia; local heating of tumors to a very high temperature using electromagnetic waves or NIR radiation.,[48] photo-dynamic therapy; utilization of photosensitizing agent and a particular type of light that produce reactive oxygen species to induce cancer cell death.,[54] gene therapy; treating the disease using small interfering RNAs (siRNA) and microRNAs (miRNA).,[64] and immunotherapy; aiding the immune system to eradicate the malignancy.[65] Interestingly, these DDSs were also shown to

be capable of taking on a combination of multiple therapeutic modalities such as chemotherapeutic drugs and gene therapy, to synergistically treat malignant tumors.[66, 67] Nonetheless, implantable biopolymeric DDSs have been commonly used in two different ways to aid in the treatment of various cancers; they can either be used as neoadjuvant or adjuvant therapies, in which the tumor itself can be treated (neoadjuvant) or the site where the tumor was removed can be treated to prevent cancer reoccurrence (adjuvant).[19]

In this paper, we will review the most recent progress in biopolymer-based DDSs for abrogating various tumors. We will specifically focus on studies with preclinical *in vivo* evidences or those with clinical evaluations, as we believe these studies are of higher value for transition of DDSs from concept to clinical application. We will further highlight various fabrication methods commonly deployed for making these DDSs and review the anti-tumor performance of some recent impressive examples. Additionally, we will evaluate future direction of anti-tumor implantable DDSs in regards to emerging biopolymers as well as cutting edge polymeric microdevices deployed as implantable anti-tumor DDSs. To conclude, a novel emerging therapeutic modality based on biopolymeric implantable DDSs for treatment of various cancers is highlighted.

2. Implantable anti-tumor DDSs

This section aims to give a brief overview of the most commonly used methods for construction of implantable DDSs and subsequently provide a comprehensive review of ensuing implantable DDSs for tumor abrogation (and prevention of tumor recurrence) in preclinical *in vivo* and clinical studies.

2.1 Preformed Implants

Owing to specific features of preformed implants, such as their structural integrity and defined geometric shapes, these implants endow predictable and adjustable long-term release and degradation profiles. *In vivo* implantation of these systems typically entails an invasive surgery.[12, 15]

2.1.1 Cast implants

Casting is considered one of the oldest fabrication methods and it can be further divided into different subcategories such as solvent casting/particulate leaching, gel casting or melt casting. Regardless of the sub category it involves pouring the polymer solution/melt into a cast and subsequently solidifying the precursor through heat/chemical or physical cross-linking/recrystallization.[68-70] One of the main perks of casting is the flexibility in choice of material as it can be easily applied to thermoplastic biopolymers (such as PLA, PLGA or PCL) as well as natural/synthetic hydrogels. Moreover, it can be utilized for fabrication of either 2D films or 3D delivery systems. [20-22, 29, 71-73] However, casting comes up short in producing structures wherein porosity, mechanical properties and/or composition as well as the distribution of these is controllable. Nevertheless, on account of its simplicity it has been widely employed for fabrication of anti-cancer DDSs from various biopolymers. [22, 71, 74]

Silk:

Silk fibroin, a protein based material, has been gaining a foothold in biomaterials science and oncology therapeutics.[75, 76] In addition to the use of silk materials for disease therapy for centuries, they are FDA approved for implantation as a bioresorbable scaffold.[77] Moreover, biodegradable materials based on silk fibroin isolated from Bombyx mori silkworm cocoons have been shown to induce minimal immune response *in vivo.*[78, 79] Consequently, it was observed that this type of protein can be combined with various anti-cancer drugs to bring about anti-tumor activity. For instance, recently, delivery of vincristine and doxorubicin (DOX) from silk foams, for treatment of neuroblastoma in a mouse model, has been investigated.[24] These implants were fabricated by lyophilization of silk solution inside a mold and subsequent thermal cross-linking at 121 ºC. The silk implants were placed intratumorally and the in vivo results revealed that silk foams loaded with vincristine, with and without DOX, significantly decreased neuroblastoma tumor growth, increased tumor drug availability and decreased ultimate plasma concentration compared to intravenous (IV) drug treatment. In another study, silk films loaded with DOX were used to suppress primary tumor growth as well as metastasis in breast cancer mice model (**Figure 3**). [22] The *in vitro* results revealed a direct correlation between absorption of DOX on silk films and silk crystallinity (beta-sheet content) that enabled controlled release of drug. The *in vivo* findings ensuing implantation of films at the primary tumor site indicated that silk films loaded with DOX had greater primary tumor response when compared to equivalent dosage of drug administered

intravenously. In addition, drug loaded stabilized films showed reduction in metastatic dissemination as a result of locoregional control of the disease.

Gelatin:

Gelatin a natural protein derived from hydrolytic degradation of collagen, has attracted much attention in the biomedical field owing to its biocompatibility and biodegradation in physiological environments.[80-82] However, gelatin has a sol-gel transition temperature around 30 ºC, and so needs to be cross-linked to avoid dissolution at body temperature.[83] Yet, in the context of cancer drug delivery this property can be leveraged to allow controlled release of the drug in a temperature-dependent manner. For example, Zhang *et al.*, made a physically cross-linked gelatin hydrogel that was embedded with poly(ethylene glycol)-block-poly(caprolactone) (PEG-b-PCL) nanoparticles ,which were co-loaded with tetrandrine (Tet) and paclitaxel (PTX), and evaluated the performance of this implant (P/T-NPs-Gelatin) for treatment of gastric cancer in mice model.[20] These hydrogel implants underwent a gradual gel-sol phase transformation at 37 ºC, which resulted in controlled release of drug loaded nanoparticles. *In vivo* results showed that P/T-NPs-Gelatin implants had the greatest inhibitory growth effect when compared to either intraperitoneal delivered P/T-NPs or free combinations of PTX and Tet. Similarly, a gelatin hydrogel loaded with gelatin/poly(acrylic acid) nanoparticles containing cisplatin (CDDP) was used for treatment of liver cancer in a murine hepatoma cancer model.[26] It was found that implantation of the gelatin hydrogel containing CDDP-loaded nanoparticles on tumor tissue led to a remarkably higher efficacy in preventing tumor growth as well as prolonged lifetime of the mice compared to that of IV injected CDDP-loaded nanoparticles. More importantly, bio-distribution results revealed that these gelatin hydrogel implants yielded a much higher drug concentration in tumor and far less accumulation in non-target organs when compared to that in the group which received systemic administered CDDP-loaded nanoparticles. Since gelatin has a variety of functional groups on its side chains, they can be exploited in various ways to crosslink the hydrogel either chemically or physically.[83] Accordingly, Jaiswal *et al.*, developed a hydrogel implant by in-situ polymerization and cross-linking of acrylic acid with polycaprolactone diacrylate in the presence of gelatin.[25] It was shown that an increase in crosslinker concentration led to a slower degradation rate as well as drug release. Additionally, the semi-interpenetrating network of gelatin and poly-(acrylic acid) loaded with DOX was implemented as an adjuvant therapy by implanting it into the tumor cavity post tumor resection to prevent recurrence of breast tumors in mice models. It was observed that use of this drug-loaded implant led to

prevention of tumor recurrence after resection until day 25 as opposed to implants with no drugs which showed tumor relapse on day 18.

Dextran:

Dextran is a polysaccharide of microbial origin consists of glucose molecules connected via a 1-6 glucosidic linkage while side chains are connected in a 1-4 linkage.[84] Aside from its biocompatibility and biodegradability, this polymer is resistant to protein adsorption and consequently it was deployed as drug delivery vehicles.[85] Owing to abundance of hydroxyl groups in this polymer, one can partially oxidize them to produce aldehyde groups that can be crosslinked by addition of amine-containing polymers.[86] For instance, based on a schiff-base interaction between dextran-aldehyde and polyamidoamine (PAMAM) dendrimers, an implantable hydrogel was made, which was embedded with poly(β-aminoester) nanoparticles containing anti-luciferase siRNA.[21] This composite hydrogel was tested *in vivo* in a xenograft mouse model for human breast cancer, and showed no sign of inflammation after implantation. All mice subjected to these implants maintained healthy conditions indicating implant biocompatibility. Furthermore, nanoparticle loaded hydrogels promoted efficient luciferase silencing, with up to 70% reduction in luciferase expression after day 6, which was significant when compared to 20% reduction of luciferase expression achieved by intratumoral injection of nanoparticles after the same period of time. Conde *et al.,* loaded the same hydrogel with dark-gold nanoparticles modified with 5-fluorouracil (5-FU)-intercalated nanobeacons, which acted as an on/off switch activated by the increase of multidrug resistance protein 1 (MPR1) within the tumor microenvironment.[66] These nanoparticles were specifically designed to detect and target MPR1 genes, a process that triggered concomitant 5-FU release following nanobeacon opening. Consequently, *in vivo* implantation of these nanoparticle loaded hydrogels resulted in over 90% tumor reduction in a triple-negative breast cancer (TNBC) mice model as a consequence of 80% MPR1 silencing.

In other work by this group, the same hydrogels were simultaneously loaded with gold nanospheres decorated with siRNAs and gold nanorods containing the anti-cancer drug bevacizumab(Avastin®), to bring about a "combinatorial" triple-combination therapy for tumor regression as well as recurrence prevention in a colon cancer mice model (**Figure 4**).[67] The gold nanospheres were designed to specifically silent a major oncogene driver (Kras) in colorectal cancer (CRC) progression, while the gold nanorods had the capacity to convert NIR radiation into heat causing release of the drug as well as photothermal therapy to ablate tumors. Accordingly, this triple therapy hydrogel (gene therapy, chemotherapy and

phototherapy combination) synergistically abrogated the tumor, and following resection it completely prevented colon cancer recurrence. Furthermore, animals which received triple therapy have shown 100% survival for at least 170 days which was significantly higher compared to control groups that received monotherapies. Conde *et al.*, also established a self-assembled hydrogel containing RNA-triple-helix to modulate miRNA in the tumor microenvironment.[64] This system was comprised of RNA-triple-helix conjugated in PAMAM G5 dendrimers (triplex nanoparticles) which formed the hydrogel upon mixing with dextran aldehyde. The RNA-triple-helix was formed by self-assembly of two miRNA oligonucleotides, an antagomiRNA used to inhibit an oncomiRNA and a miRNA mimic used as tumor suppressor. This nanoparticle loaded hydrogel were subsequently implanted in TNBC mouse models, which led to almost 90% tumor size reduction 13 days after hydrogel disk implantation, as well as a significant survival advantage in comparison to drug-loaded hydrogels. The highly selective and specific treatment of tumor cells has been shown to be the main advantage of this system over traditional chemotherapeutic drugs.

PLA and PLGA:

PLA is an US FDA approved synthetic biocompatible polymer, belonging to poly (α-hydroxy acid) class, which offers extensive mechanical properties and undergoes *in vivo* hydrolytic degradation through de-esterification.[87] However, long degradation times along with high crystallinity causing fragmentation can result in inflammatory reactions *in vivo.* Numerous methods have been used to decrease crystallinity and subsequently hasten biodegradation.[88] For instance, copolymerization of lactic acid and glycolic acid has produced PLGA with tunable degradation based on the ratio of lactic acid to glycolic acid.[89, 90] Hence, on account of desirable properties of PLGA this copolymer was extensively used in variety of clinical applications including drug delivery systems for cancer therapy.[91] For instance, Wang *et al.*, incorporated nanoparticles of RGD-modified PEGlated PAMAM dendrimer loaded with DOX (RGD-PPCD) into PLGA/PLA solution containing PEG (polyethylene glycol; as drug release modifier) and then casted them into a cylindrical die.[73] *In vitro* release studies revealed that the ratio of PLGA/PLA had an impact on the release of DOX, with an increase in PLA content decreasing the drug release rate. It was also observed that different amounts of PEG can influence the DOX release, as an increase in PEG led to significant increase in release rate of DOX. Furthermore, *in vivo* results indicated that PLG/PLA scaffolds containing RGD-PPCD nanoparticles could significantly reduce glioma tumor size in mice as opposed to their counterparts including PPCD implant, DOX implants and blank implants.

These findings were assumed to be result of better penetration of RGD-PPCD nanoparticles into the tumor which highlighted beneficial role of RGD sequence in tumor retention of nanoparticles. PLGA was also utilized to fabricate a biopolymeric cylindrical implant, known as local drug eluter (LODER), that contained an siG12D (an siRNA against the mutated KRAS oncogene) for growth inhibition of pancreatic tumors in a mouse model.[92] It was found that encapsulated siG12D in LODER was active and stable for 155 days *in vivo*. Further, it was shown that these implants were capable of impeding the tumor growth and prolonging mouse survival time. This group also conducted a phase *I* and a phase *II* clinical trials for patients with unresectable locally advanced pancreatic cancer (LAPC). The siG12D LODER implant (implanted into the tumor using an endoscopic EUS biopsy needle) was combined with chemotherapy and the results showed that from twelve patients analyzed by CT scans, none showed tumor progression and most of them (10/12) demonstrated stable disease. Tumor marker CA19-9 was observed to decrease in 70% of patients and 18 month survival rate was 38.5%.[93]

Recently, in a ground breaking study, researchers have tried to treat the pancreatic ductal adenocarcinoma (PDAC) by developing a tunable PLGA-based platform that enabled local delivery of anticancer drugs to the targeted tumor tissue (**Figure 5**).[29] Accordingly, a PLGA solution mixed with PTX was cast on top of a stainless steel disc containing a suture hole. The resulting PTX eluting device (PED) was sutured onto the tumor surface in mouse xenograft model (different PDAC cell lines with different sensitivity to PTX). The results suggested that thickness of the PLGA layer had a direct impact on PTX released, in that thicker layers yielded higher and longer release when compared against thinner layers. *In vivo* this implant showed up to 12-fold increase in suppression of tumor growth (PDAC-3 tumors with highest sensitivity to PTX), caused longer survival of mice and reduced retention in non-target organs in comparison with the group that received IV PTX. Finally, in another study, researchers have fabricated DOX loaded PLGA cylindrical millirods by casting the polymer and drug mixture into a Teflon tube via deploying heat/compression.[94] The millirods were implanted in the center of VX2 liver tumors in rabbits and the results showed that these implants were capable of significantly reducing the tumor size when compared to untreated controls. Furthermore, histological examinations revealed that necrosis happened throughout the tumor, however, some viable tumor cells were observed advancing beyond the main front of the tumor due to their lack of exposure to therapeutic drug concentration.

PCL:

PCL is yet another biocompatible polyester that has semicrystalline structure with a glass transition temperature (T_g) of -60 ºC. Therefore it has highly flexible mechanical properties at room temperature which is the reason it was extensively exploited in various biomedical applications.[95] This polymer has even slower degradation rate than PLA, due to presence of five hydrophobic $–CH_2$ moieties in its repeating unit and consequently it can be copolymerized with other hydrophilic polymers to improve its biodegradation.[96, 97] Nevertheless, owing to its slow degradation as well as its compatibility with a wide range of drugs, it was shown to facilitate drug release up to several months and it was used to fabricated anti-cancer implantable DDSs.[97]For example, injection molding was used to fabricate PCL made needle-shaped conical implants that were loaded with 5-FU to abrogate breast tumors in a mousemodel.[98] Owing to the specific design of these implants they were capable of being injected directly into the tumor using a puncture needle that eliminated the need for invasive surgery. Moreover, *in vivo* tests revealed that these implants were capable of significantly preventing tumor growth as they could provide higher regional drug concentration compared with those in mice that did not receive any treatment or only received intravenous injections of the drug.

Poly(1,3-bis-(p-carboxyphenoxy propane)-co-(sebacicanhydride))(PCPP-SA):

PCPP-SA (20:80 molar ratio) is an extremely hydrophobic copolymer that possesses surface-controlled erosion and hence it was used to fabricate Gliadel wafers for treatment of brain tumors in several clinical studies.[99, 100] These wafers were fabricated in a two-step process, where initially they were dissolved in an organic solvent along with carmustine (BCNU) and subsequently spray-dried into microparticles that were eventually made into wafers using compression molding.[4]

So far several preclinical *in vivo* studies were performed by loading these wafers with carmustine,[101] or other anti-cancer agents such as PTX,[102] 4-Hydroperoxycyclophosphamide (4-HC) [103], DOX,[104] 3-bromopyruvate (3-BrPA) and dichloracetate (DCA),[105] and subsequently implanting them intracranially against malignant glioma. For instance, one study in rat brain revealed that carmustine loaded wafers were capable of releasing carmustine over a time span of five days and they were ultimately fully degraded 6-8 weeks after implantation [101]. In another study PTX-loaded wafers were used for treatment of malignant glioma in rat brain and it was observed that PTX-loaded wafers improved the median survival of rats to different degrees depending on concentration of

loaded PTX.[102] Further, it was found that these wafers provided a much higher PTX concentration in the brain tissue proximal to the implant (75-125 ng taxol/mg brain tissue) than more distant sites (4 ng taxol/mg brain tissue). Fung *et al.,* also carried out a pharmacokinetic study on interstitial delivery of carmustine, 4-HC, and PTX from the wafers in the monkey brain which showed high drug concentration (0.5-3.5 mM for carmustine, 0.3-0.4 mM for 4-HC, and 0.2-1.0 mM for PTX) within first 3 mm from the implant and fairly lower concentration at 5 cm from the implant (0.4 µM for carmustine, 3 µM for 4-HC, and 0.6 µM for PTX) after 30 days from implantation.[103] Using area under concentration-time curve (AUC), it was also found that tissue exposure to carmustine by using implants were 4-1200 times higher than that achieved by IV administration of a higher dose. Lastly, another group of researchers investigated delivery of 3-BrPA and DCA using the wafers (both a as monotherapy or in combination with oral administration of temozolomide (TMZ) and radiation therapy (XRT)), in rat models with gliosarcoma.[105] The results showed that intracranial implantation of 5% 3-BrPA wafers and 50% DCA wafers led to significant improvement in median survival of animals, 18 days for 5% 3-BrPA wafers and 17 days for 50% DCA wafers, when compared to the control group that did not receive any treatment (13 days). Furthermore, combination of 5% 3-BrPA wafers and TMZ markedly improved the survival when compared to either therapy alone. Though triple combination therapy of wafers with TMZ and XRT did not show any statistical advantages in survival, however, 5% 3-BrPA wafers given on day 0 in combination with TMZ and XRT resulted in long-term survivorship of 30%.

In addition, numerous clinical studies for treatment of malignant glioma with gliadel wafers (as adjunct to surgery and irradiation) showed notable increase in median survival time for patients with both primary and recurrent disease [106-109], which ultimately gained these wafers FDA approval in 1997 for the treatment of recurrent malignant glioma. However, complications still remain, some of the most common side effects of these wafers in clinical trials included: seizures, intracranial hypertension, impaired neurosurgical wound healing, meningitis, wafer migration and poor drug penetration .[110, 111]

Poly(glycerol monostearate-co-ε-caprolactone) (PGC-C18):

PGC-C18 is a super-hydrophobic, biocompatible copolymer of caproic acid and glycerol functionalized with stearic acid.[112] Conjugation of hydrophobic side chains (stearic acid) imparts a large amount of hydrophobicity into this copolymer which makes it a suitable candidate for fabricating DDSs capable of delivery of anti-cancer drugs over an extended

period of time.[113] Consequently, Liu *et al.,* fabricated PTX loaded PGC-C18 polymeric films for prevention of local tumor recurrence after resection in a mouse model with lewis lung carcinoma (LLC) tumor.[72] *In vitro* drug release evaluation showed that the drug loaded film released the PTX over several weeks and *in vivo* results revealed that PTX loaded films prevented local tumor recurrence in 83.3 % of animals compared with 22.2 % for systemically administered drug. Additionally, after 10 days, drug loaded films demonstrated a significantly greater PTX concentration (3000-fold) at the site of resection when compared to that for systemic injection of PTX with equal concentration. The same group used these PTX loaded films to reduce locoregional recurrence of chondrosarcoma, in mice xenograft model, following macroscopically complete tumor resection.[71] Based on *in vivo* observations, it was found that in mice treated with PTX-loaded films locoregional recurrence was 17 % which was much lower than this value for PTX IV treated mice (89 %). Furthermore, animals treated with PTX-loaded films showed longer median overall survival (81 days) compared to PTX IV treated animals (48 days), which was due to higher concentration of PTX in the local tissue. In another study, PGC-C18 films loaded with anti-cancer agent 10-hydroxycamptothecin (HCPT) were used to prevent local growth and proliferation of LLC tumor in mice model.[114] Drug-loaded films were applied to a collagen-based scaffold to form a flexible composite that can be administered to resection margins of soft tissue via application of a surgical stapler. *In vitro*, HCPT-loaded composites released the drug over a period of seven weeks and *in vivo* observations revealed that animals treated with HCPT-loaded composites had much higher freedom from tumor growth (86 %) compared to animals that received larger intravenous dose of HCPT (0 %). Moreover, histological analysis of tissues at the surgical site showed normal wound healing process indicating the nontoxic nature of this composite.

Poly(N-isopropylacrylamide) (pNIPAAm):

poly(N-isopropylacrylamide) is a non-biodegradable polymer that due to its sharp phase transition at above 32 ºC (in pure water), has been extensively investigated in thermosreversible hydrogels.[115] This phase transition above lower critical solution temperature (LCST) is caused by a reversible conformation transition from an extended coiled state to compact globular structure, that can be observed through abrupt shrinkage of the gel.[116] The LCST of NIPAAm polymers can be tuned by copolymerizing it with monomers with different degrees of hydrophobicity; for instance, copolymerization with more hydrophobic monomer will decrease the LCST.[117, 118] Recently, NIPAAM-based hydrogels have gained attention in instituting anti-cancer DDSs. for example, a thermo-sensitive hybrid

hydrogel comprised of methoxylpoly(ethylene glycol)-poly(ε-caprolactone)-acryloyl (PECA), glycidylmethacrylated chitooligosaccharide (COS-GMA), N-isopropylacrylamide (NIPAm), and acrylamide (AAm) was synthesized (abbreviated as PCNA) and subsequently loaded with DOX and gold nanorods (GNRs) for prevention of post-operative recurrence of breast cancer (**Figure 6**).[119] A NIR laser was used to initiate the release of DOX by utilizing photothermal effect of GNRs which caused contraction of the thermo-sensitive hydrogel. *In vitro*, these hydrogels released the DOX by dual stimuli of NIR irradiation and pH. Additionally, subcutaneous implantation of composites into the mice showed complete degradation of hydrogels (due to inclusion of COS) with no inflammation after 35 days which indicated their biocompatibility. Lastly, complete resection of breast cancer tumors in mice followed by implantation of hydrogels at the original tumor site showed that after NIR irradiation DOX-PCNA-GNR hydrogels markedly reduced tumor recurrence to 16.7 %, compared with 100 % for IV DOX administration, which was assumed to be a result of synergistic effects of photothermal therapy (PTT) and chemotherapy.

Polyurethane (PU):

PU elastomers are synthesized via a reaction between isocyanates and diols to form urethane linkages (-NH-COO-) in their main chains and as a result of their biocompatibility and mechanical flexibility, they have been used in variety of biomedical applications including as anticancer DDSs.[120] For example, gemcitabine loaded PU films (GEM-PU) were used for treatment of colon cancer in a mouse model.[121] In this study, poloxamer 407 (PL) was used as a release modifier in the PU membranes (GEM-PU-PL) and it showed substantial effect on release of GEM, as membranes with higher amounts of PL demonstrated faster release when compared to the ones with lower rates of PL or pure PU. Furthermore, *in vivo* results on tumor-bearing mice revealed that implants with highest amount of PL (namely GEM-PU-PL 12%) were capable of totally inhibiting tumor-growth and even completely regress them.

Ethylene-vinyl acetate (EVA):

EVA is a biocompatible, non-degradable, inexpensive thermoplastic copolymer of ethylene and vinyl acetate (VA), which also has FDA approval.[122, 123] VA content in the copolymer plays a crucial role in determining key properties of the polymer including polarity, crystallinity and mechanical properties.[122] As a consequence of its desirable properties, drug-loaded EVA films were used as a stent coating to facilitate anti-cancer drug delivery as well

as creating physical barrier against cancer cell ingrowth.[123] For instance, a PTX or 5-FU loaded (EVA) film was developed to cover an esophageal stent for the treatment of esophageal cancer.[124] These films possessed a double layer structure where the first layer (backing layer) was composed of pure EVA film and the top layer was comprised of drug loaded EVA films, which were attached together under employment of pressure and temperature. This unique structure allowed the permeation of drug from the top layer which was in contact with the tumor tissue and prevented the leakage of drug toward the lumen of stent. *In vivo* implantation of these stents into the porcine esophagus showed that after a period of 95 days only a small amount of drug was released from the back layer of the stent, the majority of drug permeated from the top side of the film. In addition, this drug-loaded implant did not cause any systemic or local toxicity and it also inhibited the tissue response including inflammation, ulceration and hyperplasia, which indicated its potential as a nontoxic treatment modality for patients suffering from esophageal cancer.

2.1.2 Electrospun implants

Electrospinning involves the usage of a strong electric field to create fibers (with diameter ranging from micrometers down to tens of nanometers) by extruding a polymer solution from an injection needle and depositing them on a collector plate.[125-128] The electrospun fibers can vary in size and orientation (randomly distributed or aligned) based on the deployed processing parameters such as polymer solution flow rate, applied electric voltage, collector configuration (stationary or rotary), needle-tip-to-collector distance and needle size.[129, 130] As a consequence of the many interesting properties of electrospun fibers, including high specific surface area and tunable porosity, they have been frequently utilized as implantable depots for drug delivery.[125, 131, 132] One of the outstanding features of electrospinning is its ability to create multiaxial fibers comprised of a core (which can be drug loaded) and a sheath/multiple sheaths (that can retard the release of drug from the core and can also be loaded with drug) and as a result these multiaxial fibers have recently gained attention for controlled drug delivery.[133-139] Despite these properties, the use of electrospinning is limited in terms of fabrication of 3D implants with complex shapes and geometries, and not all biopolymers are spinnable with this technique.[129, 140] Nevertheless, over the past decade electrospun fibrous mats, fabricated from a variety of biopolymers, have been largely used as DDSs for abrogation of malignant tumors or preventing their reoccurrence in numerous studies.[141]

PLA and PLGA:

PLA and PLGA were shown to be ideal choices of polymers for fabrication of electrospun fibers, mainly due to their solubility in volatile chlorinated and fluorinated solvents as well as their availability in a wide range of molecular weights, which allowed ease of electrospinning of these polymers.[142, 143] Electrospun PLA and PLGA mats have been frequently used as DDSs for cancer therapy.[144] For example, electrospun PLA nanofibers that were loaded with DOX and used as local delivery systems against two types of secondary hepatic carcinoma (SHCC), namely nodular and diffuse SHCC (NSHCC and DSHCC), in mice.[31] The *in vivo* results showed that targeting NSHCC tumors with DOX loaded fibers led to significant suppression of NSHCC growth and increased the median survival time of mice with DSHCC from 14 days to 38 days. In another study, Ding *et al.,* Loaded the poly-D,L-lactide (PDLLA) nanofibers with docetaxel (DTX) to prevent breast cancer reoccurrence in mouse model.[34] It was shown that animals treated with drug loaded membranes had significant decrease in locoregional reoccurrence after primary tumor resection (16.7%) when compared to systemic administered DTX (75.0%) or local administered DTX (77.8%). Additionally these drug loaded membranes showed minimal signs of inflammation in the surrounding tissue indicating a high level of biocompatibility. Similarly, other researchers investigated the inhibitory effect of released DCA from PLA electrospun mats to suppress cervical carcinoma in tumor-bearing mice.[145] *In vivo* observations after 19 days showed a significant suppression of tumor growth in animals treated with drug loaded fibers as well as substantial reduction of tumor weight. This was assumed to be a result of synergistic necrosis of tumor cells by two different necroptosis mechanisms that were caused by high dosage of DCA. In a different study, (5-FU)-loaded PLLA nanofibrous membranes were developed for suppressing colorectal cancer in xenografted mice.[146] *In vivo* it was shown that these membranes were more capable of supressing tumor growth than an intraperitoneal injection of 5-FU (at median lethal dose (LD50) concentration) due to prolonged and continuous release of 5-FU from the membranes. PLA fibers can also be loaded with multiple chemotherapeutic agents to treat cancer in a combinatorial manner. For instance, Zhang *et al.,* evaluated the *in vivo* activity of PLA fibers containing 5-FU and oxaliplatin (Oxa) against colorectal cancer (CRC) in tumor-bearing mice.[147] As a result, it was shown that drug loaded fibers can significantly inhibit tumor growth due to higher local drug dose, caused by a sustained drug release from the fibers. Additionally, histopathological studies of the excised tumor tissue showed large areas of necrotic regions in the tumors after treatment with drug loaded fibers which was in great

correspondence with immunohistochemistry results of apoptosis related proteins (namely Bax and Bcl-2).

PLA fibers could also be arranged in a multilayer structure to bring about controlled release of the drugs. As an example, Liu *et al.,* fabricated asymmetric multilayer PLA nanofibers (AMPN) loaded with Oxa or a combination of Oxa and cyclophosphamide monohydrate (OxCy) to prevent liver cancer recurrence in mice models with either subcutaneous or orthotopic hepatocellular carcinoma (HCC).[39] Three different types of multi-layered electrospun mats were fabricated, two layered (M2), three layered (M3) and five layered (M5) (**Figure 7**). Insertion of Oxa loaded multilayered membranes into the cavity, formed as a result of "subcutaneous tumor" removal, substantially slowed the rate of tumor reoccurrence and it increased the survival rate of the rodents compared to control group. Furthermore, in orthotopic HCC models wrapping of AMPN mats (loaded with OxCy) around the left liver lobe following partial hepatectomy revealed appearance of normal liver tissue without visible tumor reoccurrence in comparison to control groups, which was further confirmed by histopathological observations of liver samples. Similarly, the same group successfully fabricated other multilayered PLA electrospun mats loaded with cisplatin or Oxa/DCA that prevented local liver cancer or cervical cancer reoccurrence in mice models, respectively.[35, 37] Last but not least, to allow loading of hydrophilic drugs into PLA-based fibers, this polymer has been mixed with more hydrophilic polymers and subsequently electrospun to make fibers with improved hydrophilicity. For instance, cisplatin loaded mucoadhesive nanofibers made out of a mixture of PLA and polyethylene oxide (PEO) were fabricated to abrogate cervical/vaginal cancer in mice.[36] Owing to the hydrophilicity properties of PEO these nanofibers showed good *in vivo* vaginal retention and upon implantation into the vagina of mice, cisplatin concentration was found to be much higher in vagina/cervix region that in the non-target organs, in contrast to the case of IV cisplatin. However, these nanofibers did not show superiority over IV cisplatin in treating vaginal tumors. Consequently, in a separate study the same group co-loaded the PLA/PEO nanofibers with cisplatin and curcumin (cis-cur) to prevent cervical cancer reoccurrence after surgery.[32] After resection of subcutaneous vaginal tumors drug loaded fibers were implanted at the site of tumor resection and it was shown that these fibers were better capable of preventing local cervical cancer reoccurrence when compared to IV drugs, which was further supported by histological analysis showing large area of necrosis induced by cis-cur/fibers only 4 days after tumor resection.

As highlighted in the beginning of this section, PLGA has also been used in fabricating anti-cancer fibrous DDSs. For example, Ranganath *et al.,* fabricated submicron (F2) and nanoscale (F3) discs from PLGA(50:50) electrospun fibers loaded with PTX and used them for inhibiting growth of glioblastoma in a mouse model.[148] Consequently, F3 nanofibrous discs demonstrated a greater drug release rate *in vitro* and *in vivo*, in comparison to counterparts including F2 submicron fibrous discs and PTX-loaded PLGA microspheres entrapped in sodium alginate beads. As a result, F3 discs showed higher drug availability and subsequently enhanced diffusion rate as well as diffusion distance in the mouse brain tissue that is crucial considering that glioblastoma multiforme (GBM) typically reoccurs within 2 cm of the resection site. Moreover, F3 discs were capable of inhibiting the tumor at its early stages of tumor growth as a consequence of high local drug concentration, which is critical to slow down the reoccurrence rate of glioma in post-surgical chemotherapy. In another study carried out by Tseng *et al.,* PLGA nanofibrous membranes were loaded with combination of drugs including BCNU, irinotecan and cisplatin to treat malignant glioma in tumor-bearing rats.[149] Consequently, in rats treated with drug loaded fibers (BIC/PLGA), a substantially higher concentration of drugs was observed in brain tissue than in the blood throughout 8 weeks of study. Rats treated with BIC/PLGA membranes experienced a much lower tumor volume after 16 days, when compared to that in rats which received blank PLGA membranes. Furthermore, in the BIC/PLGA treated group a much longer median survival time was achieved (~60 days) in comparison to the group treated with non-drug loaded (blank) membranes (~22 days).

PCL:

Due to specific rheological and viscoelastic properties of PCL this polymer and its copolymers have been successfully utilized in electrospinning to bring about fibrous mats.[150] Similar to PLA and PLGA, PCL fibers were also utilized as drug carriers for local delivery of anti-cancer drugs to tumor site. For instance, Chen *et al.,* made nanofibers from combination of PCL and gelatin (PG), that contained DOX-loaded core-shell nanoparticles of Cu_9S_5-mesoporous SiO_2 (Cu_9S_5@$mSiO_2$) and used them for synergistic chemo- and photothermal therapy of hepatoma tumors in mice (**Figure 8**).[151] *In vitro* DOX release in PBS (phosphate-based buffer) revealed that these fibrous membranes possessed pH responsive release owing to intrinsic properties of Cu_9S_5@$mSiO_2$ nanoparticles, also, it was shown that after 5 min laser irradiation the temperature of Cu_9S_5@$mSiO_2$ PG fibers dramatically increased from 21 ºC to 54.6 ºC. Additionally, *in vivo* results showed that DOX-loaded Cu_9S_5@$mSiO_2$ PG composite

fibers under laser irradiation had a more efficient tumor suppression effect once compared against single photothermal therapy of tumors by Cu_9S_5@$mSiO_2$ PG fibers or with single chemotherapy by Dox loaded Cu_9S_5@$mSiO_2$ PG fibers. In another study the same group fabricated similar PG nanofibers instead loaded them with DOX-containing NaGdF4:Yb/Er@NaGdF4:Yb@mSiO2-PEG core-shell nanoparticles (upconverting nanoparticles; UCNPs) and indomethacin (anti-inflammatory drug) to abrogate hepatoma tumors in mice.[33] This composite fiber not only was aimed for controlled-release of DOX but also enabled upconversion fluorescence/magnetic resonance dual-modality imaging via NaGdF4:Yb/Er@NaGdF4:Yb incorporated into composite fibers. *In vivo* anti-tumor efficacy showed that composite fibers containing DOX-loaded UCNPs and indomethacin had the highest tumor inhibition rate (96%) when compared to simple DOX-loaded fibers (61.8%). Moreover, owing to presence of indomethacin in composite fibers, they caused complete healing of surgical wound. At last, in an attempt to further prolong the drug release of PCL nanofibers, researchers fabricated cisplatin-loaded superhydrophobic electrospun nanofibers from mixture of PCL and Poly(caprolactone-co-glycerol-monostearate) (PGC-C18) for prevention of local cancer reoccurrence post resection in mice model with lung carcinoma.[152] Owing to hydrophobicity of these nanofibers they have shown a sustained release of drug over 90 days. Further, *in vivo* evaluation showed that these fibers were capable of significantly increasing median reoccurrence-free survival rate to more than 23 days compared to the group treated with intraperitoneal injection of cisplatin which all died before day 16 due to cancer recurrence.

Gelatin:

Owing to superior biocompatibility and biodegradability of gelatin, this polymer was extensively utilized to fabricate electrospun fibers (either alone or as a blend component) for various biomedical applications including drug delivery.[131, 153] For instance, Yang *et al.,* fabricated core-shell fibers, in which the core was comprised of polyvinyl alcohol (PVA) containing folate-decorated micelles (FM) of poly(ε-caprolactone)-poly(ethylene glycol) loaded with DOX (for active targeting of solid tumors), and the shell contained genipin crosslinked gelatin (**Figure 9**).[139] These fibers showed delayed *in vitro* release of DOX when compared with micelles alone, and further *in vivo* studies in mice with breast cancer revealed that DOX accumulation in tumors for FM (IV administrated) and FM-nanofiber groups (implanted near the tumor) were significantly higher than that in DOX treated (IV administrated) group. Moreover, during 21 days of treatment, groups treated with FM-

nanofiber showed comparable tumor growth suppression in comparison to the groups that received four times injection of DOX or M or FM. Lastly, FM-nanofiber treated group experienced a higher survival rate when compared to other groups, owing to lower systemic drug exposure caused by local delivery of DOX using the nanofibers.

Polyurethane (PU):

On account of biocompatibility and excellent mechanical properties of PU electrospun fibers, they have been recently exploited as anti-cancer DDSs. For instance, a PTX-eluting polyurethane electrospun membrane was fabricated for inhibiting the growth of colon cancer in a tumor-bearing mouse model.[154] These PTX-eluting nanofiber membranes (PTX-NFM) showed sustained release of PTX for 30 days in both PBS buffer and PBS buffer with bile extract. Additionally, implantation of these fibers next to colon carcinoma tumors in mice resulted in significant inhibition of tumor growth when compared with the group treated with sub-tumoral injection of PTX (PTX-INJ). Moreover, mice treated with PTX-NFM showed sustained intratumoral concentration of PTX until 21 days after implantation in contrast to PTX-INJ treated group which showed almost no PTX within tumor tissue only 7 days after injection.

2.1.3 3D printed implants

3D printing is known as a process whereby three dimensional solid objects of any shape are constructed from a computer-aided design (CAD) model via layer-by-layer deposition of materials onto a computer-controlled built platform.[127, 155] Technically, 3D printing encompasses various technologies such as inkjet printing, microextrusion printing, laser-assisted printing, stereolithography and fused deposition modeling (FDM), and they all offer significant advantages over traditional fabrication methods as they endow reliability, reproducibility and flexibility in design (geometrically complex shapes).[155-157] In the context of cancer studies 3D printing has been used to recreate the 3D microenvironment of tumors by printing a variety of hydrogels and this aspect of 3D printing will not be reviewed here.[158-160] Herein, we solely focus on bipolymeric anti-cancer drug eluting implants fabricated using 3D printing technologies.

3D printed DDSs are commonly fabricated via microextrusion or FDM printing.[161] Microextrusion printing involves continuous extrusion of biomaterials (in the form of solution/paste) from a temperature-controlled micro-extrusion head to a building platform,

using pneumatic pressure or piston-assisted system, for layer-by-layer fabrication of 3D constructs.[127, 162] FDM deploys preformed filaments fed into a temperature-controlled extruder where they are heated and subsequently the semi-molten thermoplastic is deposited onto a platform in a layer by layer process.[163, 164] Such printing is directly affected by processing parameters such as nozzle diameter and temperature, feed rate and print head speed.[165, 166] Interlayer bonding significantly affects the final properties of the printed product and consequently solidification procedures should be carefully controlled to avoid separation of subsequent layers. The major disadvantages of extrusion and FDM printing include: slow printing speed, nozzle clogging and interlayer debonding.[167] Even so, these methods have been successfully practiced on biopolymers such as PCL and PLGA to fabricate implantable anti-cancer DDSs.

PLGA and PCL:

Owing to the thermoplastic nature of PCL and PLGA in conjunction with their favorable biocompatibility and biodegradability, they have been utilized to create 3D printed DDSs for cancer therapy. For example, most recently extrusion printing was used to fabricate a 3D patch made from a mixture of PLGA (lactide:glycolide = 85:15) and PCL loaded with 5-FU for growth suppression of pancreatic cancer (**Figure 10**).[27] The patches were printed with three different pore shapes and geometries (latticed, slant and triangular) in different thicknesses and it was found that these features can greatly affect the drug release profile by altering the surface area:volume ratio (S:V) of the structure. Implantation of drug-loaded patches (P100;100 mg 5-FU and P150;150 mg 5-FU) underneath a pancreatic cancer tumor in mice, resulted in a substantial decrease in tumor size when compared to non-drug loaded patch (P0) groups. In another study, Sun and his colleagues fabricated a PCL scaffold using a FDM printer and coated the structure with a mixture of chitosan, chitosan-modified montmorillonite clay and β-tricalcium phosphate (β-TCP) which was subsequently coated with DOX solution (DESCLAYMR_DOX) to inhibit growth of breast tumors in mice .[28] These drug eluting implants showed a significant burst release of DOX in the first 24 h that was followed by four weeks of sustained release. Further, subcutaneous implantation of DESCLAYMR_DOX in mice showed prolonged presence of DOX to a much larger extent at the treatment site which resulted in higher tumor growth inhibition when compared to subcutaneous injection of DOX (INJECTION_DOX). Also compared to INJECTION_DOX,

DESCLAYMR_DOX showed decreased multi-organ metastasis as well as cardiotoxicity due to local delivery of DOX.

2.2 Injectable in-situ forming implants

Injectable DDSs are typically made from a solution/semisolid mixture of polymer matrix and therapeutic agents that solidify *in situ* upon injection into the tumor site. [10, 15, 168] The solidification mechanism will differ based on the type of biopolymer used, however, the existing injectable DDSs can be generally categorized accordingly[168-170]: (*I*) *in situ* precipitation, wherein the polymer precipitates from a solution state as a consequence of solvent removal [171, 172], sol-gel transition in response to temperature change[40, 41, 43] or pH change[42, 173]; (*II*) *in situ* crosslinking, wherein the polymer chains undergo physical/chemical cross-linking upon injection as a result of covalent bonding [53, 55, 174-177] , or non-covalent bonding of polymeric chains.[50, 51, 54] The injectable implants hold great advantages over preformed implants including elimination of invasive surgical intervention and their ability to fill any cavity, into which they are injected.[178-180] Some of the disadvantages of these implants are the complicated and sometimes toxic crosslinking chemistry required as well as the fairly long gelation time upon injection.[168] Nevertheless, recently injectable DDSs, developed from a broad range of biopolymers, have been extensively used to inhibit the growth of malignant tumors or prevent their recurrence in preclinical and clinical studies.[181]

Polyethylene glycol *(PEG):*

PEG is a FDA-approved synthetic hydrophilic polymer that has various structures including linear and branched (multi-arm or star-shaped).[182] Aside from its desirable properties such as good biocompatibility and non-immunogenity, this polymer is capable of being chemically modified with various functional groups (via replacement of two hydroxyl groups in its repeating unit) to provide certain functionalities.[183, 184] Consequently, PEG and its copolymers have been frequently used to bring about injectable DDSs based on either *in situ* precipitation or *in situ* crosslinking mechanisms. PEG-based injectable hydrogels established via *in situ* precipitation are often thermo-gelling hydrogels that have been synthesized via copolymerization of PEG with other polymers to allow sol-gel transition of the hydrogel upon changes in temperature. For instance, DOX-loaded nanoparticles made from copolymer of poly(ε-caprolactone-co-1,4,8,trioxa[4.6]spiro-9-undecanone)-poly(ethylene glycol)-poly(ε-caprolactone-co-1,4,8, trioxa[4.6]spiro-9-undecanone) (PECT) have formed the macroscale

hydrogel upon thermo-sensitive self-aggregation of PECT/DOX nanoparticles at 37 °C in aqueous media (**Figure 11**).[41] Peritumoral injection of PECT/DOX hydrogel into the breast tumors of mice showed a much higher intratumoural concentration of DOX when compared to other organs, which in turn led to greater suppression of tumor growth. In addition, survival rate increased in animals treated with PECT/DOX hydrogel compared to ones who received IV injection of DOX or PECT/DOX NPs, which was largely due to the fact that hydrogels were capable of locally releasing DOX within the tumor area, preventing distribution of DOX to other organs. Researchers developed another thermo-sensitive hydrogel from MPEG-b-(PCL-PLLA) diblock copolymer loaded with 5-FU that underwent an instantaneous sol-gel transition at body temperature.[185] Intratumoral injection of this system into melanoma tumors in mice showed higher tumor suppression effect and subsequent necrosis of tumor tissue which was comparable to that of mice who received three intratumoral injections of free 5-FU, each at equivalent concentrations to that of one hydrogel injection. Similarly, Phan *et al.,* synthesized a thermo-sensitive triblock copolymer of poly(ε-caprolactone-co-lactide)-b-poly(ethylene glycol)-b-poly(ε-caprolactone-co-lactide) (PCLA-PEG-PCLA) that was used to develop an injectable hydrogel containing nanoparticles of montmorillonite loaded with gemcitabine (MMT-GEM).[186] Interestingly, the targeted injection of this composite hydrogel into a pancreatic tumor (in mice) led to enhanced anti-tumor efficacy when compared to control group of intratumorally injected GEM solution at equivalent concentrations.

Triblock copolymers of PLGA and PEG (PLGA-PEG-PLGA) are specifically attractive thermo-responsive systems on account of their biodegradability and acceptable safety profile and they showed to undergo sol-gel transition at physiological temperature (37 °C).[187] As a result, this copolymer has been exploited as delivery systems for anti-cancer drug delivery purposes.[188, 189] As an example, incorporation of DOX into this thermo-gel did not interfere with its sol-gel transition (except at high concentration of DOX; 4 mg/ml) and after injection of this drug loaded hydrogel in the vicinity of a sarcoma-tumor in mice, significant suppression of tumor growth as well as strong apoptosis of tumor cells were achieved. [190] Similarly, Zhang *et al.,* used the same DOX loaded PLGA-PEG-PLGA thermo-gel and injected it into hepatic-tumor in mice.[191] Interestingly, similar anti-tumor efficacy was observed in this case and toxicity studies revealed that these drug loaded hydrogels caused mild lesions in major organ tissues (heart, liver, spleen lung and kidney) when compared with DOX control group. The same gel was also loaded with PTX, also known as OncoGel, and used as palliative therapy in pre-clinical *in vivo* studies in rats with metastatic spinal tumors,[192] mice with breast carcinoma [193] and porcine model for future application in non-

resectable pancreatic ductal adenocarcinoma.[194] Most importantly, a phase I clinical trial on patients with superficially accessible advanced solid tumors and a phase 2a clinical study on patients with inoperable esophageal cancer (OncoGel used in adjuvant to radiotherapy), showed that OncoGel administered intralesionally was well tolerated, retained its position at the site of injection and caused low systemic concentration of PTX.[195, 196] Other types of PEG-based thermo-gelling copolymers include triblock copolymer of poly(ethyleneglycol)-poly(ε-caprolactone)- poly(ethyleneglycol) (PEG-PCL-PEG, PECE) and triblock copolymer of poly(γ-ethyl-L-glutamate)-poly(ethylene glycol)-poly(γ-ethyl-L-glutamate) (PELG-PEG-PELG). Both these copolymers form a gel quickly after being exposed to body temperature and they have been employed for local delivery of anti-cancer drugs in animal models.[197, 198] For instance, Lei *et al.,* loaded PECE with PTX and injected it at the original tumor site in 4T1 breast cancer -bearing mice, with the intention of preventing locoregional recurrence of primary tumor after resection.[47] As a result, recurrence of the tumor was significantly inhibited by administration of PTX-loaded PECE hydrogels (9.1%) compared with systemic (77.8%) or local (75%) administration of PTX at an equivalent concentration. In addition, this hydrogel accelerated post-operative wound healing at the surgical incision site, indicating its superior biocompatibility. In another work, Cheng *et al.,* loaded PELG-PEG-PELG thermo-gels with PTX and used it for local delivery of PTX to liver carcinoma in mice models.[199] Interestingly, it was shown that by adjusting the length of each block in the copolymer a different sol-gel transition temperature could be achieved. Injection of PTX loaded PELG-PEG-PELG hydrogel beside the tumor revealed enhanced tumor growth suppression when compared to equivalent amounts of free PTX and higher anti-tumor activity that was confirmed by TUNEL staining of apoptotic cells.

As it was highlighted at the beginning of this section PEG can also be used to bring about injectable hydrogels based on *in situ* crosslinking. This normally involves functionalization of PEG with a variety of desirable functional groups, which are either mixed with a secondary polymer to facilitate the cross-linking, or can be used alone to enable radical/photo cross-linking of the PEG chains.[200, 201] For instance, Wang *et al.,* used polydopamine nanoparticles (PDANPs) to cross-link thiol-terminated four-arm PEG (via thiol-ene reaction) and form a hydrogel that showed sensitivity towards NIR irradiation, owing to the presence of polydopamine (**Figure 12**).[177] This feature was further used for controlled release of the drug as well as photothermal therapy of tumors. Upon intratumoral injection of 7-ethyl-10-hydroxycamptothecin (SN38) loaded gel into a lung cancer mouse model, it was found that

PDA-SN38/PEG gel with NIR radiation had greater anti-tumor activity when compared with the PDANP-SN38 group, due to synergistic interactions of the the chemo- and photothermal therapy. In addition, these gels caused no detectable pathological change in major organs indicating their minimal systemic toxicity. In another study, a heparin functionalized four-arm PEG hydrogel was synthesized which was further processed post-synthesis into injectable microparticle aggregates.[49] Owing to the presence of heparin in these hydrogel microparticles they have shown high affinity towards DOX especially at higher concentrations, leading to slow *in vitro* release of this drug in PBS. Moreover, local injection of the DOX-loaded hydrogel microparticles into established human orthotopic breast tumours in miceshowed significant reduction in tumor burden as well as breast cancer metastasis when compared to IV bolus-treated animals. Li *et al.,* used acylhydrazone bonds to form a pH-sensitive injectable hydrogel from a mixture of dibenzaldehyde-terminated PEG (DF-PEG) and polyaspartylhydrazide (PAHy).[42] *In vitro*, these hydrogels showed faster release of DOX in a buffer solution with acidic pH compared to a neutral pH due to cleavage of acylhydrazone bonds in acidic conditions. Furthermore, intratumoral injection of DOX-loaded hydrogel in fibrosarcoma tumor bearing mice showed a superior antitumor activity compared to control groups as well as negligible toxicity *in vivo*.

Guest-host interactions have also been implemented to make PEG-based injectable hydrogels based on *in situ* crosslinking mechanism. For example, Kuang and his coworkers synthesized two types of nucleobase-terminated PEG (adenine and thymine) that upon mixing with α-cyclodextrin (α-CD) formed an injectable hydrogel based on guest-host interactions.[50] Additionally, intratumoral injection of DOX loaded hydrogel into a cervical cancer mouse model revealed that this hydrogel substantially restricted the tumor growth and caused no significant fluctuation in body weight (compared to control groups) which was assumed to be a consequence of slow and longer local release of DOX from this hydrogel. Similarly, the concept of guest-host interaction was used by another group to make an injectable biocompatible hydrogel by developing a mixture of methoxy polyethylene glycol (MPEG) conjugated with arginine-functionalized poly(L-lysine) Dendron and α-CD (MPEG-PLLD-Arg), for delivery of MMP-9 short hairpin RNA plasmid (pMMP-9).[52] *In vitro*, these hydrogels were capable of sustained release of pMMP-9 and after intratumoral injection of drug-loaded hydrogels in nasopharyngeal carcinoma tumor-bearing mice, it was shown that MPEG-PLLD-Arg/pMMP-9 hydrogels enhanced retention of pMMP-9 in the tumor compared to standard pMMP-9-loaded Polyethylenimine (PEI-25K/pMMP-9). Moreover, one

time injection of this new hydrogel had equivalent anti-tumor efficiency to seven injections of a conventional PEI-25K/pMMP-9 that totalled the plasmid concentration in the hydrogel.

Wu *et al.,* designed another injectable hydrogel based on Schiff-base interaction of aldehyde-functionalized four-arm PEG (PFA) and 4-arm poly(ethylene glycol)-b-poly(L-lysine) (PPLL) for co-delivery of metformin (ME) and 5-FU.[55] *In vitro* drug release and degradation studies showed that this hydrogel released both ME and 5-FU in a pH-sensitive manner. Moreover, a single subcutaneous injection injection of the drug loaded hydrogel (ME and 5-FU) beside the tumors of BALB/c mice bearing colon adenocarcinomas led to significant anti-tumor activity compared to that of single and combination bolus drug doses, and this was a result of p53-mediated G_1 arrest and apoptosis of tumor cells caused by synergistic therapeutic effect of ME and 5-FU. Additionally, histological assessment of major organs in mice that were treated with blank (non-drug loaded) hydrogel revealed their excellent biocompatibility. And lastly, a photo-crosslinkable hydrogel made from polyethylene glycol dimethacrylate (PEG-DMA) was used for delivery of temozolomide-loaded polymeric micelles (M-TMZ) to brain tumors in mice.[176] Drug-loaded hydrogel was intracranially injected into a human glioblastoma bearing xenograft mouse model and subsequently photo-crosslinked *in situ*. It was shown that the unloaded hydrogel did not cause any apoptosis in the brain of the mice, while the drug loaded hydrogel markedly decreased the tumor weight when compared to all the other control groups. Furthermore, histological analysis of tumors (retrieved seven days post-treatment) using CD34 and Ki67 staining, revealed that mice treated with *in situ* cross-linked drug-loaded hydrogel showed no sign of cancer proliferating cells at the center of tumor but were present at the periphery.

Pluronic F-127 (poloxamer 407):

Triblock copolymers of poly(ethylene oxide)-poly(propylene oxide)-poly(ethylene oxide) (PEO-PPO-PEO) have been of great interest in drug delivery due to their gelation phenomenon,[202-207] however among them pluronic F127 is reported to be the least toxic one and it also showed inhibitory effect against P-glycoprotein, a major player in the multidrug-resistant phenotype in cancer.[169, 208, 209] As a result, this polymer has gained much interest as DDS against malignant tumors.[210-216] For instance, three different types of thermo-sensitive F-127 hydrogels were developed with either paclitaxel (PTX) in the form of molecules (MOs), nanocrystals (NCs) and microcrystals (MCs).[40] Interestingly, *in vitro* erosion and release studies showed very small release of PTX from PTX-NCs-Gel and PTX-MCs-Gel whilst PTX-MOs-Gel showed the highest amount of release after 14 days in PBS which was in direct

correlation with their corresponding erosion rates. In addition, it was shown that PTX-MCs-Gel possessed the highest intratumoral drug concentration followed by PTX-NCs-Gel and PTX-MOs-Gel, respectively. Lastly, PTX-NCs-Gel showed the highest anti-tumor efficacy against breast tumor xenografts in mice when compared with PTX-MCs-Gel and PTX-MOs-Gel, which was assumed to be a consequence of sustained release of drug from PTX-NCs-Gel. In a separate study, Chen *et al.*, attempted to improve the mechanical properties of pluronic F-127 by copolymerzing it with hexamethylene diisocyanate (HDI-PF127) and subsequently mixing it with hyaluronic acid (HDI-PF127/HA).[43] Hence, the mentioned hydrogel showed a sol-gel transition at 37 °C and after intratumoral injection of DOX-loaded gels in breast tumor-bearing mice, it was shown that DOX-loaded HDI-PF127/HA gel exhibited the highest tumor growth inhibition compared to DOX-loaded PF127/HA gel due to its slower degradation rate and controlled DOX release. Finally, Guo *et al.,* synthesized linoleic acid (CLA)-couple poloxamer (CLA-c-P) thermo-sensitive hydrogel to benefit pro-drug activity of CLA and further increase stability of the hydrogel.[46] Injection of PTX-loaded CLA-c-P hydrogel beside breast cancer tumor in mice model led to significant suppression of tumor growth when compared with control groups, as a result of the synergistic effect of CLA in conjugation with PTX. Moreover, significant reduction in expression of cell cycle signaling proteins (Cyclin A, Cyclin B, Cyclin D_3 and CDK2) in combination with considerable increase in expression level of pro-apoptic protein caspase 3 verified cancer cell death *in vivo*.

Poly(N-isopropylacrylamide) (pNIPAAm):

As highlighted previously, pNIPAAm has recently attracted attention as a DDS for cancer treatment, mainly due to its phase transition from a hydrated state to a collapsed state above its LCST. However, this polymer by itself is not suitable to be used as injectable implants, mainly because injection of highly elastic hydrogels is impractical.[217] Consequently, in order to give shear thinning behavior to this hydrogel, it was copolymerized or functionalized with secondary polymers, which also improved the biodegradability of the resulting gel. [218] Nevertheless, pNIPAAm-based injectable hydrogels have lately gained a foothold in drug delivery.[219-221] For example, Zhou *et al.,* developed a DOX loaded thermo-sensitive injectable hydrogel (with LCST of 33 °C) by attaching amine-terminated pNIPAAm to gelatin modified-single wall carbon nanotube (SWNT) and used this hydrogel for chemo-phototermal treatment of gastric cancer in a xenograftin mouse model of disease.[219] *In vitro* this hydrogel showed a sustained release of DOX in PBS over a period of 28 days. *In vivo* experiments revealed that DOX loaded SWNT-GEL accompanied by NIR radiation had the highest tumor

growth inhibition compared to free DOX group (injected intratumorly) or SWNT-GEL group without NIR radiation, as a consequence of synergistic effect of DOX and hyperthermia. Furthermore, Hoechst (HE) staining of four major organs (heart, liver, kidney, spleen) after 28 days of treatments with SWNT-GEL, showed no apparent organ damage, indicating good biocompatibility of this gel. Similarly, Xu and his colleagues, made a smart injectable nanocomposite hydrogel by copolymerizing NIPAAm and DOX loaded methacrylated poly-β-cyclodextrin (MPCD), in presence of gold nanorods (GNRs), and subsequently used it for chemo-photothermal synergistic therapy of sarcoma in a mouse model.[220] It was shown that mass ratio of monomers in the copolymer had a major effect on LCST of the resulting hydrogel. *In vitro* experiments in PBS revealed that the nanocomposite hydrogels were capable of releasing DOX in response to pH change or NIR radiation. Moreover, *in vivo* observations showed that animals treated with DOX loaded gel+NIR radiation experienced outstanding tumor growth suppression when compared with free DOX group, which was further confirmed by histopathological analysis of treated tumor tissues.

Collagen:

Collagen one of the most abundant proteins in the human body, has been extensively explored for biomedical applications.[222] Collagen can undergo self-assembly to form injectable fibrous hydrogel based on non-covalent bonding.[223] Consequently, collagen has gained attention as an injectable DDS for a variety of cancers. For example, a collagen peptide modified dendrimer attached to DOX via a hydrazone bond (CP-Dox-den) was synthesized and embedded in collagen gel. [224] Subsequent injection of this gel underneath a breast cancer tumor (in mice) led to prolonged suppression of tumor growth. Additionally, CP-Dox-den/Col gel was even capable of suppressing metastasis in tumor-bearing mice, as a result of sustained release of DOX from the gel over the period of the experiment. Peng *et al.*, designed another injectable hydrogel from a mixture of collagen and Polyethylenimine (PEI) containing ld1-targeted siRNA for gastric cancer inhibition.[225] Consequently, collagen/PEI-siRNA gels showed slower and sustained release of siRNA owing to better stability of these gels compared to collagen-siRNA gels. Additionally, *in vivo* anti-cancer studies using a gastric cancer xenograft mouse model revealed that collagen/PEI-siRNA gel inhibited tumor growth to a greater degree compared with collagen-siRNA gels or siRNA/medium, which was further confirmed by immunostaining of treated tumor cells with cell-cycle antibodies (cyclin D1 and P21) and cell proliferation antigen (PCNA). Most recently, researchers developed an

injectable hydrogel from a mixture of collagen and gold nanoparticles (AuNPs) containing a photosensitizer (PS) for non-invasive combinational photodynamic therapy (PDT) and photothermal therapy (PTT) of breast cancer in mice (**Figure 13**).[54] This hydrogel was formed due to ionic interactions of negatively charged $[AuCl_4]^-$ ions with positively charged collagen. Intratumoral injection of this hydrogel into tumor-bearing animals followed by irradiation using laser light resulted in up to an 80% elimination rate of tumors. In addition, the dual therapy caused suppression of tumor recurrence for a longer period of time when compared to monotherapies, denoting superior synergistic anti-cancer effect of photodynamic therapy and photo thermal therapy.

Cisplatin/Epinephrine (CDDP/epi) gel is also an injectable hydrogel based on collagen matrix and it was exploited in several clinical studies in patients with esophageal cancer,[226] adenocarcinomas,[227] squamous cell carcinomas [228] and hepatocellular Carcinoma.[229] For instance, Monga *et al.,* injected the CDDP/epi gel intratumorally (using endoscopy) in nine patients with esophageal cancer and it was found that this treatment restored swallowing in 8 of nine patients, highlighting its palliative-therapy potential. [226]

Chitosan:

Chitosan is a cationic linear polysaccharide composed of randomly distributed β-(1-4)-linked D-glucosamine and N-acetyl-D-glucosamine units, and on account of its intrinsic properties such as, biocompatibility, biodegradability, penetration enhancer (opening epithelial tight-junction) and wound healing promoter, has received great deal of attention in medical and pharmaceutical applications.[230, 231] Injectable chitosan-based hydrogels are generally made by neutralization of chitosan amine groups that eliminates the repulsive inter-chain electrostatic forces and allows development of extensive hydrogen bonding and hydrophobic interactions between chains, which eventually leads to formation of hydrated gel-like precipitate.[232] Furthermore, it was shown that pH sensitive chitosan gels can be transformed into thermally sensitive gels by addition of polyol salts such as β-glycerophosphate (GP).[116]

Injectable chitosan-based gels have shown great promise in local delivery of anti-cancer drugs. For instance, a thermo-sensitive injectable hydrogel containing chitosan and β-glycerophosphate (C/GP) loaded with liposomal doxorubicin (LipDOX) was developed and showed pH-dependent release of DOX in *in vitro* settings.[233] *In vivo* results from intratumoral injection of this gel into liver tumor-bearing mice showed that LipDOX+C/GP had a better anti-tumor effect and less systemic cytotoxicity when compared with DOX+C/GP gels, due to more sustained release of DOX from LipDOX+C/GP which caused a larger

therapeutic window. In another study, Hsiao *et al.*, synthesized a chitosan derivative, which contained self-doped acid substituted polyaniline (PANI) side chain (NMPA-CS) that was capable of self-assembling into a micellar hydrogel upon local pH change (sol-gel transition at pH of 7).[173] Interestingly, exposing NMPA-CS solution to NIR laser showed rapid increase in its temperature (to 54 °C) within 5 min of exposure and possessed excellent photostability. Subsequently, subcutaneous injection of this gel into the right flank of mice showed mild foreign-body reaction with slow degradation. Additionally, intratumoral injection of NMPA-CS in liver cancer-bearing mice followed by NIR radiation (5 min every 4 days) led to effective suppression of tumor growth and maintained no sign of tumor progression for the duration of study, as a consequence of successful photothermal therapy of these tumors. Shi coworkers also made an injectable pH-sensitive hydrogel resulting from Schiff-base interaction of succinated chitosan (S-chi) and oxidized alginate (O-alg).[174] This hydrogel showed faster *in vitro* release of DOX at lower pH in PBS and subsequent intratumoral injection of DOX loaded hydrogel (DOX-OS) in a xenograft mouse model of breast cancer resulted in greater and longer inhibition of tumor growth when compared to the DOX-treated control group.

Hyaluronic acid:

Hyaluronic acid (HA) is a biocompatible, biodegradable non-sulfated glycosaminoglycan which has been largely used over the years for drug delivery purposes.[234] Injectable hyaluronic acid-based hydrogels can be formed using various methods, including Schiff-base reaction and covalent crosslinking with secondary agents.[235] For instance, an injectable hydrogel based on physical cross-linking of hyaluronic acid/adipic acid dihydrazide (HA-ADH) and hyaluronic acid aldehyde (HA-CHO) was developed and subsequently loaded with two types of paclitaxel, namely microparticulate paxlitaxel (PTX) and 14 nm micelle form of PTX (Taxol).[236] Consequently, *in vitro* PTX-gel showed slower release of paclitaxel compared to Taxol-gel as a result of smaller particle size of PTX. In addition, treatment of ovarian cancer in a xenograft mouse model with these hydrogels revealed significant reduction in tumor burden compared to control group, however no significant difference between tumor burden of mice treated with PTX-gel or Taxol-gel was observed, which was assumed to be a result of limited dissolution of PTX. Cho *et al.*, developed a similar hydrogel and loaded them with platinum incorporated HA nanoparticles (PtNPs) and upon injection of this gel into the peritoneal cavity of ovarian cancer -bearing mice found that PtNP/gel and PtNP were not capable of inhibiting tumor growth and proliferation at later time points due to

pro-tumorigenic effect of HA in the DDS.[53] In a different study, Ueda *et al.,* designed an injectable hydrogel from interferon-alpha (IFN-α)-incorporated hyaluronic acid-tyramine (HA-Tyr) through oxidative coupling of Tyr with hydrogen peroxide (H_2O_2) and horseradish peroxide (HRP). [237, 238] The IFN-α-incorporated HA-Tyr gel was further combined with sorafenib (a small molecule tyrosine kinase inhibitor) for synergistic anti-cancer effect in a renal carcinoma xenograft mouse model. It was found that IFN-α-incorporated HA-Tyr gel+sorafenib caused the highest inhibition of tumor growth, which was further confirmed by the ratio of apoptotic cells and Ki-67-positive cells in the treated tumors. This synergistic effect was attributed to induction of apoptosis in conjugation with suppression of angiogenesis by IFN-α-incoporated HA-Tyr gel+sorafenib hydrogel.

Alginate:

Alginate a naturally occurring anionic polysaccharide has been extensively studied in tissue engineering and drug delivery avenues on account of its ideal biocompatibility and adjustable gelation properties.[239, 240] Alginate-based injectable hydrogels can be made by exploiting a variety of chemistries including non-covalent bonding such as ionic bonds, schiff-base interactions and acylhydrazone Bonds.[240] Ionic cross-linking of alginate chains with divalent cations such as Ca^{2+} provides a facile route to development of injectable formulations of this polymer. For instance most recently, Wang *et al.,* developed an injectable alginate-calcium hydrogel with immobilized acetylated G5-NH_2 PAMAM dendrimer-encapsulated platinum nanoparticles (D_{Ac}EPts) in its matrix for non-invasive photothermal ablation of tumors.[51] This hydrogel was capable of being degraded on-demand upon addition of a chelator (diethylene triamine pentacetic acid-DTPA). Intratumoral injection of D_{Ac}EPts containing hydrogel (H/D_{Ac}EPts) in lung cancer -bearing immunocompromised mice followed by NIR irradiation led to significant decrease in tumor volume compared to controls after 30 days of treatment. Interestingly, in the D_{Ac}EPts treated group, tumor-site temperature did not stay stable due to leakage of these nanoparticles out of the tumor tissue, however, the H/D_{Ac}EPts treated group showed maintenance of temperature at 47 °C after each NIR irradiation. Additionally, after two intratumoral injections of the DTPA chelator (at day 9 and day 12) the liberated D_{Ac}EPts nanoparticles leached form the tumor tissue, which in turn resulted in an attenuated efficiency of the hydrogel in terms of tumor growth suppression.

Poly(organophosphazene):

Poly(organophosphazene) is an inorganic/organic hybrid polymer that has immense potential for biomedical applications as a result of its hydrolytic degradability and non-toxic degradation products.[241, 242] Furthermore, this hydrogel undergoes a sol-gel transition in psychological temperature that makes it a suitable candidate for anti-cancer injectable DDSs. For example, Al-Abd *et al.*, loaded the poly(organophosphazene) thermogel with DOX for local delivery of this drug to human gastric tumor xenografts in mice.[243] Interestingly, it was observed that DOX loaded gel (POL) had 40% and 90% sustained drug release over 5 weeks *in vitro* and *in vivo*, respectively. *In vivo* results suggested that POL had similar efficacy in suppressing tumor growth as DOX loaded solution (SOL), however POL showed dramatically decreased systemic toxicity compared to SOL leading to higher survival rates of animals after 28 days of treatment. In a different study, Zhang *et al*., synthesized poly(organophosphazene) nanocapsules loaded with superparamagnetic iron-oxide nanoparticle that transformed to a hydrogel (SPION-NHs) upon exposure to body temperature and it was further used for magnetic hyperthermia (MHT) and long-term magnetic resonance imaging (MRI).[48] Intratumoral injection of SPION-NHs in human brain cancer tumor xenograft in mice showed higher retention of SPION nanoparticles in the tumor tissue compared with that in the group treated with PEGylated SPIONs solution. Moreover, it was shown that treatment cycles of multiple MHT using SPION-NHs has a direct effect on tumor regression as mice treated with one or two cycles of MHT demonstrated resumed tumor growth after 5 days of treatment, however, mice treated with four cycles of MHT showed significant tumor eradication. Finally, long-term MRI monitoring of tumors injected with SPION-NHs showed dissipation of SPIONs from the tumor site as a result of apoptosis of tumor cells. Similarly, the same group loaded the SPION-NHs hydrogel with tumor necrosis factor-related apoptosis-inducing ligand (TRAIL) (T/S-NHs) to synergistically abrogate tumors by multiple MHT and anti-cancer potential of TRAIL.[244] Accordingly, it was shown that chemical structure of poly(organophosphazene) (PPZ) had a direct effect on *in vitro* degradation and subsequent release of TRAIL and SPIONs from the hydrogel, as nonionic side group on PPZ (indicated as T/S-NHs-1) led to fastest degradation rate as well as fastest SPIONs and TRAIL release, while, hydrogel made from PPZ with ionic side groups (indicated as T/S-NHs-2 and T/S-NHs-3) showed much slower degradation rate and consequently slower TRAIL and SPIONs release. Additionally, intratumoral injection of T/S-NHs in a glioblastoma tumor xenograft in mice revealed that tumor growth was significantly inhibited in animals that received T/S-NHs-2 with two cycles of MHT as a result of combinational therapy.

PLGA:

PLGA, an FDA approved thermoplastic biopolymer, has also been deployed to generate injectable DDSs for cancer treatment because of its quick in-situ precipitation in aqueous environment. For instance, Chen *et al.,* incorporated the iron(III) oxide (Fe_3O_4) nanoparticles into a PLGA solution for magnetic-hyperthermia regression of tumors.[172] Intratumoral injection of this solution in a breast cancer xenograft mouse model followed by only single magnetic ablation showed complete disappearance of the tumor after 3 days and without reoccurrence even after 1 month. The same group also developed another injectable DDS based on PLGA, which MoS_2 nanosheets and DOX were incorporated into the implant for synergistic photothermal and chemotherapy of tumors (**Figure 14**). [171] Therefore, this implant showed controlled release of DOX in pH- and NIR- responsive manner. Furthermore, intratumoral injection of this composite in a breast cancer tumor xenograft mouse model followed by only one time NIR irradiation (5 min) led to disappearance of tumor after 7 days and no tumor recurrence was observed within 2 months from the treatment. Lastly, mice treated with PMD+NIR had 100 % of survival rate over a period of 50 days, which indicated high efficiency of this local synergistic treatment.

3. Future trends

In the following sections, we will briefly highlight some of the recent trends in anti-tumor polymeric implantable DDSs with special emphasis on emerging biopolymers as well as state-of-the-art implantable anti-cancer micro-devices. Furthermore, a novel therapeutic modality, based on biopolymeric implantable DDSs for treatment of various cancers is highlighted.

3.1 Emerging biopolymers

Recent advances in biopolymers have brought about new generations of biopolymers with peculiar characteristics such as self-healing,[223, 245-247] photoluminescence,[175] and thermo-degradability,[248, 249] that have greatly contributed to development of novel multi-functional anti-cancer DDSs.

Self-healing

Stability of implants after implantation is of great importance particularly considering its direct effect on corresponding drug release profile. Hence, DDSs that can autonomously heal themselves upon damage and restore the integrity and functionality of DDS have recently gained much attention.[223, 245-247] Worth noting that self-healing implantable DDSs are often made from hydrogels based on either dynamic covalent bonds or non-covalent bonds, which allow reversible formation of hydrogel network.[250] For example, Wang *et al.,* developed an injectable self-healing hydrogel from a mixture of glycol chitosan, telechelic difunctional poly (ethylene glycol) (DF-PEG) and saline ions that were used for microwave tumor ablation.[245] Periodic step-strain experiment (2 cycles of 1% then 300% strain) showed that the hydrogel was capable of recovering 100% of storage modulus almost instantly. The intrinsic self-healing capability of this hydrogel stemmed from Schiff base bond between amino groups of chitosan and benzaldehyde groups of DF-PEG. *In vivo* biocompatibility study demonstrated only a mild foreign-body reaction indicating good biocompatibility. Intratumoral injection of DOX loaded hydrogel in glioma tumor xenograft (in mice), in combination with microwave treatment led to effective suppression of tumor growth within 14 days that was further confirmed with histological assessment of tumors *ex vivo*. Similarly, Yang *et al.,* used the same hydrogel in combination with PTX and intratumoral injection of this DDS in liver cancer tumor xenograft (in mice) showed significant inhibition of tumor growth when compared to that in mice that received Pluronic F127 hydrogel loaded with PTX.[246] This observation was assumed to be the result of unique self-healing ability of the hydrogel allowing it to rebuild as a whole after injection which prevented the leak of PTX and subsequently resulted in longer-term anti-tumor efficacy.

In a recent effort, Xing *et al.,* made a self-healing, shear-thinning hydrogel based on electrostatic interactions between positively charged collagen chains and anionic cluster of [$AuCl_4$] ions that subsequently formed gold nanoparticles (AuNPs) in the gel.[223] Continuous step-strain test (3 cycles of 1% and then 500% strain) showed that the broken structure recovered rapidly and demonstrated normal hydrogel-like behavior. Intratumoral injection of hydrogel showed persistent retention in a breast tumor xenograft (in mice) and subsequently displayed sustained release of model drug (Meso-Tetra (N -methyl-4-pyridyl) porphine tetrachloride/ TMPyP) within the tumor site. Intratumoral injection of the hydrogel followed by laser irradiation showed suppression of tumor proliferation depending on number of treatment cycles, as animals that received one cycle of irradiation showed initial tumor volume decline, followed by rapid tumor growth 5 days post treatment, whereas, animals that

received five cycles of irradiation showed delayed tumor growth and even tumor eradication after 23 days. lastly, Huebsch *et al.*, fabricated a self-healing alginate hydrogel that was cross-linked with calcium sulfate.[247] The polysaccharide was cross-linked by divalent cations (Ca^{2+}) and it was observed that ultrasound was capable of disrupting ionic cross-linking to accelerate mitoxantrone release, while Ca^{2+} ions in physiological fluids allowed cross-links to reform after removal of the ultrasound (**Figure 15A**). Interestingly, *in vitro* studies using MDA-MB-231 and MCF7 breast cancer cell lines revealed that ultrasound-mediated pulsatile release of mitoxantrone had significantly higher anti-tumor activity when compared with sustained release of drug from the same hydrogel. Injection of this hydrogel adjacent to MDA-MB-231 tumor xenografts in mice followed by ultrasound treatment of animal showed higher inhibition of tumor growth as well as higher survival rate when compared to those in mice treated with systemic exposure of drug or drug-loaded gel without ultrasound.

Photoluminescence:

Fate of polymeric DDSs after implantation is vital for patient's compliance to therapy.[251] Hence, traditionally fluorescent dyes have been incorporated into DDSs to allow optical tracking of these systems, however, fluorescent dyes are potentially toxic and eventually leak out of the DDS.[252] On the other hand, sericin based (a major component of natural silk) hydrogel was found to exhibit excellent photoluminescence as well as *in vivo* biocompatibility.[253] Consequently, Liu *et al.*, developed an injectable hydrogel, from a mixture of sericin functionalized with adipic acid dihydrazide (Sericin-ADH) and dextran dialdehyde (DEX-Al), for use as an optically trackable DDS for treatment of malignant melanoma **(Figure 15B)**.[175] The hydrogel was formed based on hydrazone bonds between amino groups of sericin-ADH and carbonyl groups of DEX-Al. Photoluminescence of hydrogels were observed under two excitation wave lengths of 405 and 488 nm. After subcutaneous injection of these gels into dorsal skin of mice, they were readily detected and visualized with excitation wavelength at 405 nm and emission wavelength at 530 nm. Moreover, it was shown that there was a direct correlation between degradation of the hydrogels and their corresponding fluorescence intensity. Ultimately, injection of DOX-loaded gels in the vicinity of a melanoma tumor in mice led to increased tumor growth suppression and prolonged survival time once compared with the groups treated with free DOX.

Thermo degradation:

Thermo-sensitive biopolymers have been extensively used in the field of drug delivery to fabricate DDSs that undergo sol-gel transition above their lower critical solution temperature (LCST).[118, 254] However, recently a new generation of thermo-sensitive biopolymers were explored that can undergo degradation and/or chain dissociation after being exposed to heat.[13] This feature can be further used to allow on demand delivery of therapeutic agents via administration of heat. For instance, Hu *et al.,* designed a thermo-responsive injectable hydrogel by cross-linking four-arm amine-terminated poly(ethylene glycol) with an azo-containing linker and the hydrogel showed rapid degradation above 44 °C due to breakage of azo bonds (**Figure 15C**).[248] Embedding this hydrogel with photothermal nanoparticles (dendritic platinum-copper nanoparticles) enabled on-demand and dose-tunable release of entrapped DOX *in vitro* upon irradiation with NIR light. *In vivo* Injection of this hydrogel under the dorsal skin of nude mice followed by NIR irradiation (once per day for 10 min) degraded the majority of hydrogel mass after 3 days of treatment. Finally, intratumoral injection of DOX loaded gel into breast tumor xenografts (in mice) followed by NIR irradiation led to significant regression of tumor volume as a result of fast release of DOX in the tumor site. Wang *et al.,* synthesized a different thermo-degradable injectable hydrogel composed of PEG-modified PAMAM dendrimer encapsulated with platinum nanoparticles (DEPt-PEG) and alpha-cyclodextrin (α-CD).[249] The linear PEG chains threaded into a series of CD cavities via a well know host-guest interaction, to form pseudopolyrotaxane (PPR) assemblies and subsequently strong hydrogen bonding among the adjacent threaded CDs promoted physical gel formation. Interestingly, the threading-dethreading transition is a thermosensitive phenomenon that facilitated on-demand degradation of the hydrogel. The DEPt-PEG/α-CD hydrogel showed a temperature increase up to 46 °C only after 5 min of NIR irradiation, and was observed that hydrogel degradation had a direct correlation with duration of NIR irradiation. *In vitro*, bortezomib loaded hydrogels were capable of markedly abrogating human lung cancer cells after NIR irradiation and further, subcutaneous injection of fluorescent dye (cyanine 5.5)-loaded hydrogel in mice exhibited much higher dye release after NIR radiation, which suggested that thermo-degradation of this hydrogel can be used for on-demand delivery of drugs.

3.2 Anti-cancer polymeric micro-devices

Recent efforts to institute miniaturized drug delivery devices has ultimately led to development of integrated systems that incorporated device technology with therapeutic molecules to create implantable devices capable of disease treatment *in situ*.[255-257] Based on the design of these micro-devices they could present different options such as allowing continuous or intermittent delivery, operating for short or long periods.[255] Similar to traditional DDSs, these devices can either exert passive delivery of a drug or they can permit real-time control of drug dosage by means of external stimulus.[258] In the following section, some of the most salient examples of polymeric micro-devices for cancer therapy are reviewed.

Jonas *et al.,* recently engineered a small cylindrical device (via micro-machining from a medical grade acetyl resin blocks) designed to release a wide range of anti-cancer drugs from 16 discrete reservoirs on its perimeter (**Figure 16A**).[259] The device was directly implanted into tumors of different types using a biopsy procedure and left in there for 24 h for quick, parallel investigation of drug sensitivity in *in vivo* tumors. Next, the device and a small region of tissue were removed using a coring biopsy needle, to determine the anti-neoplastic effect of each treatment. In order to modify the release rate of each drug in the reservoir, three different techniques were used: (1) altering the size of reservoir opening, (2) embedding drugs into polymeric matrix (PEG) and (3) using a hydrophilic expansive polymer that would expand upon contact with fluid in the tumor in order to deliver hydrophobic drugs. Consequently, It was shown that the device was capable of delivering individual or combination (co-delivered from one reservoir or delivered separately from two adjacent reservoirs) of drugs into confined regions of tumor tissue. The authors further evaluated the pharmacokinetics of DOX release from the device in human breast carcinoma tumor xenografts and it was shown that the drug released from device can diffuse 200 to 300 μm into tumor tissue. In addition, this device was found to be useful in combatting tumor heterogeneity (a major challenge in all diagnostics) by implanting a device, with sixteen identically loaded reservoirs (with DOX) on different locations of the device, in the non-necrotic periphery of skin cancer tumor xenografts.

Dosage of drug and frequency of its administration play a crucial role in the treatment of chronic diseases such cancer.[260, 261] Consequently, advanced techniques that allow on demand, precise and controlled local delivery of drugs are highly needed for individualized disease treatment.[262] Owing to digital capabilities of microelectromechanical systems

(MEMS) they allow for complex temporal profiles, while the manufacturing techniques used in microelectronic industry can lead to greater device uniformity and reproducibility than currently available to pharmaceutical and biomedical industries.[263-266] On account of such desirable features MEMS devices have been recently explored for anti-cancer drug delivery purposes and have shown some promising results.[265, 267, 268]. However, the major issues with MEMS devices are related to biocompatibility of materials used to institute the device as well as constant need for a sustained power supply. Consequently, in a notable effort Chin *et al.,* used photolithography to develop a biocompatible and biodegradable MEMS micro-device from PEG diacrylate (PEGDA), which contained moving parts that can be controlled by an external magnet (**Figure 16B**).[268] Specifically, two different designs of this device, single-gear and geneva drive, were tested *in vivo* on a mouse model. Single-gear device contained a multi-reservoir gear, where one of them was loaded with iron oxide nanoparticles (NPs) and the others with drugs. On the other hand, geneva drive had two engaged gears, a driving gear that was doped with iron oxide NPs and a driven gear with six drug loaded reservoirs. The concept of release for both designs were the same, where movement of an external magnet caused motion in the gears (owing to presence of NPs) and the drug in each reservoir was released once the aperture on top it aligned with another aperture on topmost layer of the assembled device. Subcutaneous implantation of the geneva drive device (in a mouse model) loaded with two different fluorescent dyes showed successful movement of gears *in vivo* which led to controlled release of the dyes. Furthermore, the DOX-loaded single gear device (loaded with 10% of a single standard chemotherapy dose) was implanted adjacent to a human osteosarcoma xenograft (in a mouse model), which was actuated once every 2 days, over a period of 10 days. Consequently, this showed the greatest tumor volume reductions with the presence of tumor necrosis, and also caused the lowest levels of cardiotoxicity compared to all other treatment groups (including systemic administration of various concentrations of DOX with different frequencies). Lastly, analysis of the excised device and surrounding tissue showed no signs of chronic inflammation and revealed normal wound healing indicating good biocompatibility of this device.

3.3 Emerging therapeutic modality based on biopolymeric implantable DDSs

Considering the versatility of implantable biopolymeric DDSs, it allows them to be loaded with novel anti-cancer therapeutic agents to deliver high concentrations to the disease site. Therefore, in this section we will briefly discuss a recently emerging therapeutic modality to abrogate primary tumors and subsequently bring examples of implantable biopolymer-based DDSs that were used to deliver these agents directly to the tumor.

Cancer immunotherapy

Cancer immunotherapy involves any intervention that aids the immune system to eradicate a malignancy.[269] Immunotherapy modalities can function via two different mechanisms, either by stimulation of the intrinsic immune system or by unleashing extrinsic immune system components such as specific proteins to be recognized and targeted by immune cells.[9] However, multiple factors have hampered the success of these therapies in clinical cases including; associated toxicity, difficulties involved with defining the optimal dosage and schedule of immunotherapy and at last lack of efficiency in patients with a large tumor burden.[9, 270, 271] Biomaterial based systems, however, are capable of addressing these issues owing to their intriguing properties such as protecting the bioactive agents or cells, exerting control over their spatiotemporal release and competency to deliver more than one agent from a single platform.[272] Consequently, a wide range of biomaterials have been used for delivery of immunomodulatory factors and here we will only highlight the most recently developed implantable bio-polymeric DDSs used for this purpose. In the context of cancer immunotherapy these implantable DDSs can be used in two well distinguished ways, either for delivering immunomodulatory agents that override checkpoints in the cancer-immunity cycle or to deliver cells for adoptive cell transfer (ACT) into cancerous tissue to enhance their survival and proliferation.[273]

Delivery of immunomodulatory factors

Many types of immunomodulatory agents, antibodies, antigens, adjuvants, cytokines and checkpoint inhibitors have been loaded into implantable bio-polymeric DDSs to provide immune-protection against cancer.[274] For example, Bencherif and his colleagues developed a methacrylated alginate (MA-alginate) sponge-like cryogel containing covalently conjugated RGD peptide which was encapsulated with GM-CSF (granulocyte-macrophage colony-

stimulating factor), CpG ODN (cytosine-phosphodiester guanine oligodeoxynucleotide) and irradiated tumor cells (B16-F10 mouse skin melanoma cells).[275] Subcutaneous injection of this cryogel vaccine into a mouse model brought about a durable and specific anti-tumor T-cell response which led to 80% survival rate in a B16-F10 tumor model. Moreover, it was shown that cryogel vaccines bestow long lasting protective immunity as 100% of vaccinated mice that survived the initial tumor challenge survived the subsequent second challenge.

Delivery of cells for ACT

ACT offers great advantages over other methods of cancer immunotherapies, which heavily rely on *in vivo* recruitment of a sufficient number of antitumor T cells with required functions to instigate cancer regression.[276] Usually in ACT a large pool of antitumor lymphocyte, capable of recognizing tumor cells, are grown and proliferated *in vitro* and subsequently administered to the patient with the aim of providing a tumor microenvironment that supports antitumor immunity.[277] Nevertheless, recent years have witnessed emergence of bio-polymeric scaffolds as platforms for improving function of these adoptive cells and enabling their local delivery to the tumor site. [269, 278] For example, Stephan *et al.*, developed a bioactive polymeric carrier designed for expanding and delivering tumor-reactive T cells for treating inoperable or incompletely removed tumors in a mouse breast cancer resection model (**Figure 17**).[65] The microporous scaffolds were made of alginate functionalized with collagen-mimetic peptide (used to facilitate migration of T cells through the scaffolds by means of α2β1 collagen receptor) using ionic crosslinking. Furthermore, porous silica microparticles containing anti-CD3, anti-CD28 and anti-CD137 antibodies were incorporated into the scaffold to create stimulatory microenvironment for cytotoxic T-lymphocytes (CTL) proliferation. For *in vivo* studies breast cancer xenografts in mice were intentionally partially resected to mimic reoccurrence post-resection. Ultimately, implantation of these scaffolds at the resection site led to higher T cell proliferation and consequently none of the treated mice showed tumor reoccurrence after a period of 80 days, in contradiction to the control group which all died due to cancer relapse. In another study Aliperta and his colleagues reported a macroporous cryogel scaffold made from four-arm poly(ethylene glycol)-heparin that were used for housing gene-modified human mesenchymal stromal cells (MSCs), capable of secreting anti-CD33-anti-CD3 bispecific antibody (bsAb), for treatment of acute myeloid leukemia (AML).[279] This scaffold supported the proliferation and survival of bsAb-releasing-MSCs and was observed to secret bsAb in a sustained manner both *in vitro* and *in vivo*. For purpose of *in vivo* anti-tumor evaluation, leukemia tumor cells ($CD33^+$ MOLM-13 cells) were

injected into right leg of mice and the scaffolds were subcutaneously implanted into the left leg. Consequently, it was shown that sufficient amount of released bsAb reached circulation leading to efficient redirection of T cells to CD33 positive AML cells and causing significant reduction in tumor size.

4. Conclusion

Despite a steady decrease in cancer mortality over the last few decades, the current standards of care in cancer treatment encounter major obstacles in efficiently treating the disease. Therefore, bio-polymeric implantable DDSs have been designed to overcome hurdles faced by conventional therapies, by means of local delivery of therapeutic agents directly to the tumor site. These DDDs have consequently shown immense promise in treating malignant tumors (or preventing disease recurrence) in animal models as well as in some clinical cases. Not only do these DDSs possess intriguing properties (such as biocompatibility, biodegradability and trackability) but they are also capable of delivering a variety of anti-cancer therapeutic agents while exerting precise spatiotemporal control over their release. More importantly, in multiple cases these DDSs were shown to be useful for combinational therapy of tumors, using chemotherapeutic drugs in conjugation with either hyperthermia or photodynamic therapy or gene therapy. Nevertheless, in order for bio-polymeric implantable DDSs to reach a broad clinical implementation, scientists have to discover simple polymer chemistries that are easy to follow while offering sufficient safety. Lastly, continual communication between scientists and clinicians is crucial for establishing new treatment standards, based on the cancer type and stage, which would lead to optimal therapeutic and patient outcomes.

Acknowledgements

This work has been supported by the Australian Research Council under the Discovery Early Career Researcher Award (J. Foroughi, DE130100517) and the authors would like to acknowledge funding from ARC Laureate Fellowship (FL110100196) and the Center for Medical and Molecular Bioscience and the Faculty of Science Medicine and Health (2015/SPGT-S/07), University of Wollongong.

References:

[1] M. Larsson, W.-T. Huang, D.-M. Liu, D. Losic, Cancer Treatment Reviews 2017.
[2] D. Hanahan, Robert A. Weinberg, Cell 2011, 144, 646.
[3] J. Conde, N. Shomron, N. Artzi, Advanced Healthcare Materials 2016, 5, 2312.
[4] J. B. Wolinsky, Y. L. Colson, M. W. Grinstaff, J. Controlled Release 2012, 159, 14.
[5] K. D. Miller, R. L. Siegel, C. C. Lin, A. B. Mariotto, J. L. Kramer, J. H. Rowland, K. D. Stein, R. Alteri, A. Jemal, CA: a cancer journal for clinicians 2016, 66, 271.
[6] J. Conde, N. Shomron, N. Artzi, Advanced Healthcare Materials 2016.
[7] T. M. Allen, P. R. Cullis, Science 2004, 303, 1818.
[8] R. De Souza, P. Zahedi, C. J. Allen, M. Piquette-Miller, Drug delivery 2010, 17, 365.
[9] S. A. Chew, S. Danti, Advanced healthcare materials 2016.
[10] A. Santos, M. S. Aw, M. Bariana, T. Kumeria, Y. Wang, D. Losic, Journal of Materials Chemistry B 2014, 2, 6157.
[11] C. McConville, Australian Pharmacist 2011, 30, 764.
[12] B. D. Weinberg, E. Blanco, J. Gao, J. Pharm. Sci. 2008, 97, 1681.
[13] C. J. Kearney, D. J. Mooney, Nature materials 2013, 12, 1004.
[14] C. Bastiancich, P. Danhier, V. Préat, F. Danhier, J. Controlled Release 2016, 243, 29.
[15] K. Krukiewicz, J. K. Zak, Materials Science and Engineering: C 2016, 62, 927.
[16] S. Doppalapudi, A. Jain, A. J. Domb, W. Khan, Expert opinion on drug delivery 2016, 1.
[17] S. J. Wade, A. Zuzic, J. Foroughi, S. Talebian, M. Aghmesheh, S. E. Moulton, K. L. Vine, Pancreatology 2017, 17, 795.
[18] L. W. Kleiner, J. C. Wright, Y. Wang, J. Controlled Release 2014, 181, 1.
[19] A. A. Exner, G. M. Saidel, Expert opinion on drug delivery 2008, 5, 775.
[20] H. Zhang, Y. Tian, Z. Zhu, H. Xu, X. Li, D. Zheng, W. Sun, Scientific reports 2016, 6.
[21] N. Segovia, M. Pont, N. Oliva, V. Ramos, S. Borrós, N. Artzi, Advanced healthcare materials 2015, 4, 271.
[22] F. P. Seib, D. L. Kaplan, Biomaterials 2012, 33, 8442.
[23] C.-C. Huang, W.-T. Chia, M.-F. Chung, K.-J. Lin, C.-W. Hsiao, C. Jin, W.-H. Lim, C.-C. Chen, H.-W. Sung, J. Am. Chem. Soc. 2016, 138, 5222.
[24] J. Coburn, J. Harris, A. D. Zakharov, J. Poirier, N. Ikegaki, A. Kajdacsy‐Balla, M. Pilichowska, A. V. Lyubimov, H. Shimada, D. L. Kaplan, International journal of cancer 2017, 140, 726.
[25] M. Jaiswal, F. Naz, A. K. Dinda, V. Koul, Biomedical Materials 2013, 8, 045004.
[26] D. Ding, Z. Zhu, R. Li, X. Li, W. Wu, X. Jiang, B. Liu, ACS nano 2011, 5, 2520.
[27] H.-G. Yi, Y.-J. Choi, K. S. Kang, J. M. Hong, R. G. Pati, M. N. Park, I. K. Shim, C. M. Lee, S. C. Kim, D.-W. Cho, J. Controlled Release 2016, 238, 231.
[28] M. Sun, M. Wang, M. Chen, F. Dagnaes-Hansen, D. Q. S. Le, A. Baatrup, M. R. Horsman, J. Kjems, C. E. Bünger, Acta biomaterialia 2015, 18, 21.
[29] L. Indolfi, M. Ligorio, D. T. Ting, K. Xega, A. R. Tzafriri, F. Bersani, N. Aceto, V. Thapar, B. C. Fuchs, V. Deshpande, Biomaterials 2016, 93, 71.
[30] Y. Ramot, S. Rotkopf, R. M. Gabai, E. Zorde Khvalevsky, S. Muravnik, G. A. Marzoli, A. J. Domb, A. Shemi, A. Nyska, Toxicologic pathology 2016, 44, 856.
[31] S. Liu, G. Zhou, D. Liu, Z. Xie, Y. Huang, X. Wang, W. Wu, X. Jing, Journal of Materials Chemistry B 2013, 1, 101.
[32] Y. Ma, X. Wang, S. Zong, Z. Zhang, Z. Xie, Y. Huang, Y. Yue, S. Liu, X. Jing, RSC Advances 2015, 5, 106325.
[33] Y. Chen, S. Liu, Z. Hou, P. Ma, D. Yang, C. Li, J. Lin, Nano Research 2015, 8, 1917.
[34] Q. Ding, Z. Li, Y. Yang, G. Guo, F. Luo, Z. Chen, Y. Yang, Z. Qian, S. Shi, Drug delivery 2016, 23, 2677.

[35] Y. Zhang, S. Liu, X. Wang, Z.-y. Zhang, X.-b. Jing, P. Zhang, Z.-g. Xie, Chin. J. Polym. Sci. 2014, 32, 1111.
[36] S. Zong, X. Wang, Y. Yang, W. Wu, H. Li, Y. Ma, W. Lin, T. Sun, Y. Huang, Z. Xie, European Journal of Pharmaceutics and Biopharmaceutics 2015, 93, 127.
[37] Z. Zhang, S. Liu, Y. Qi, D. Zhou, Z. Xie, X. Jing, X. Chen, Y. Huang, J. Controlled Release 2016, 235, 125.
[38] X. Zhao, Z. Yuan, L. Yildirimer, J. Zhao, Z. Y. W. Lin, Z. Cao, G. Pan, W. Cui, Small 2015, 11, 4284.
[39] S. Liu, X. Wang, Z. Zhang, Y. Zhang, G. Zhou, Y. Huang, Z. Xie, X. Jing, Nanomedicine: Nanotechnology, Biology and Medicine 2015, 11, 1047.
[40] Z. Lin, D. Mei, M. Chen, Y. Wang, X. Chen, Z. Wang, B. He, H. Zhang, X. Wang, W. Dai, Nanoscale 2015, 7, 14838.
[41] P. Huang, H. Song, Y. Zhang, J. Liu, J. Zhang, W. Wang, J. Liu, C. Li, D. Kong, ACS Applied Materials & Interfaces 2016, 8, 29323.
[42] L. Li, J. Gu, J. Zhang, Z. Xie, Y. Lu, L. Shen, Q. Dong, Y. Wang, ACS applied materials & interfaces 2015, 7, 8033.
[43] Y.-Y. Chen, H.-C. Wu, J.-S. Sun, G.-C. Dong, T.-W. Wang, Langmuir 2013, 29, 3721.
[44] C. T. Huynh, Q. V. Nguyen, J. S. Lym, B. S. Kim, H. J. Jae, Y. I. Kim, D. S. Lee, RSC Advances 2016, 6, 47687.
[45] Z.-Q. Zhang, S.-C. Song, Biomaterials 2017.
[46] D.-D. Guo, C.-X. Xu, J.-S. Quan, C.-K. Song, H. Jin, D.-D. Kim, Y.-J. Choi, M.-H. Cho, C.-S. Cho, Biomaterials 2009, 30, 4777.
[47] N. Lei, C. Gong, Z. Qian, F. Luo, C. Wang, H. Wang, Y. Wei, Nanoscale 2012, 4, 5686.
[48] Z.-Q. Zhang, S.-C. Song, Biomaterials 2016, 106, 13.
[49] F. P. Seib, M. Tsurkan, U. Freudenberg, D. L. Kaplan, C. Werner, ACS Biomaterials Science & Engineering 2016.
[50] H. Kuang, H. He, Z. Zhang, Y. Qi, Z. Xie, X. Jing, Y. Huang, Journal of Materials Chemistry B 2014, 2, 659.
[51] C. Wang, X. Wang, K. Dong, J. Luo, Q. Zhang, Y. Cheng, Biomaterials 2016, 104, 129.
[52] Q. Lin, Y. Yang, Q. Hu, Z. Guo, T. Liu, J. Xu, J. Wu, T. B. Kirk, D. Ma, W. Xue, Acta biomaterialia 2017, 49, 456.
[53] E. J. Cho, B. Sun, K.-O. Doh, E. M. Wilson, S. Torregrosa-Allen, B. D. Elzey, Y. Yeo, Biomaterials 2015, 37, 312.
[54] J. Sun, Y. Guo, R. Xing, T. Jiao, Q. Zou, X. Yan, Colloids and Surfaces A: Physicochemical and Engineering Aspects 2017, 514, 155.
[55] X. Wu, C. He, Y. Wu, X. Chen, Biomaterials 2016, 75, 148.
[56] I. Tokarev, S. Minko, Soft Matter 2009, 5, 511.
[57] J. Hu, H. Meng, G. Li, S. I. Ibekwe, Smart Mater. Struct. 2012, 21, 053001.
[58] P. Bawa, V. Pillay, Y. E. Choonara, L. C. Du Toit, Biomedical materials 2009, 4, 022001.
[59] B. P. Timko, T. Dvir, D. S. Kohane, Adv. Mater. 2010, 22, 4925.
[60] S.-k. Ahn, R. M. Kasi, S.-C. Kim, N. Sharma, Y. Zhou, Soft Matter 2008, 4, 1151.
[61] K. E. Uhrich, S. M. Cannizzaro, R. S. Langer, K. M. Shakesheff, Chem. Rev. 1999, 99, 3181.
[62] Y. Fu, W. J. Kao, Expert opinion on drug delivery 2010, 7, 429.
[63] X. Huang, C. S. Brazel, J. Controlled Release 2001, 73, 121.
[64] J. Conde, N. Oliva, M. Atilano, H. S. Song, N. Artzi, Nature materials 2016, 15, 353.
[65] S. B. Stephan, A. M. Taber, I. Jileaeva, E. P. Pegues, C. L. Sentman, M. T. Stephan, Nat. Biotechnol. 2015, 33, 97.

[66] J. Conde, N. Oliva, N. Artzi, Proceedings of the National Academy of Sciences 2015, 112, E1278.
[67] J. Conde, N. Oliva, Y. Zhang, N. Artzi, Nature Materials 2016.
[68] U. Siemann, Scattering Methods and the Properties of Polymer Materials 2005, 307.
[69] H. J. Chung, T. G. Park, Advanced Drug Delivery Reviews 2007, 59, 249.
[70] C. Agrawal, R. B. Ray, Journal of biomedical materials research 2001, 55, 141.
[71] R. Liu, J. B. Wolinsky, P. J. Catalano, L. R. Chirieac, A. J. Wagner, M. W. Grinstaff, Y. L. Colson, C. P. Raut, Annals of surgical oncology 2012, 19, 199.
[72] R. Liu, J. B. Wolinsky, J. Walpole, E. Southard, L. R. Chirieac, M. W. Grinstaff, Y. L. Colson, Annals of surgical oncology 2010, 17, 1203.
[73] K. Wang, X. Zhang, L. Zhang, L. Qian, C. Liu, J. Zheng, Y. Jiang, Drug delivery 2015, 22, 389.
[74] S.-G. Kang, S. C. Lee, S. H. Choi, S. Park, S. Jeong, D. H. Lee, M. Kim, Macromolecular research 2010, 18, 680.
[75] K. Jastrzebska, K. Kucharczyk, A. Florczak, E. Dondajewska, A. Mackiewicz, H. Dams-Kozlowska, Reports of Practical Oncology & Radiotherapy 2015, 20, 87.
[76] B. Kundu, R. Rajkhowa, S. C. Kundu, X. Wang, Advanced Drug Delivery Reviews 2013, 65, 457.
[77] T. Yucel, M. L. Lovett, D. L. Kaplan, J. Controlled Release 2014, 190, 381.
[78] A. E. Thurber, F. G. Omenetto, D. L. Kaplan, Biomaterials 2015, 71, 145.
[79] C. Vepari, D. L. Kaplan, Prog. Polym. Sci. 2007, 32, 991.
[80] D. Olsen, C. Yang, M. Bodo, R. Chang, S. Leigh, J. Baez, D. Carmichael, M. Perälä, E.-R. Hämäläinen, M. Jarvinen, J. Polarek, Advanced Drug Delivery Reviews 2003, 55, 1547.
[81] M. Santoro, A. M. Tatara, A. G. Mikos, J. Controlled Release 2014, 190, 210.
[82] M. Mehrali, A. Thakur, C. P. Pennisi, S. Talebian, A. Arpanaei, M. Nikkhah, A. Dolatshahi‐Pirouz, Adv. Mater. 2017, 29.
[83] S. Van Vlierberghe, P. Dubruel, E. Schacht, Biomacromolecules 2011, 12, 1387.
[84] V. Sinha, R. Kumria, Int. J. Pharm. 2001, 224, 19.
[85] A. K. A. Silva, M. Juenet, A. Meddahi-Pellé, D. Letourneur, Carbohydr. Polym. 2015, 116, 267.
[86] S. G. Lévesque, R. M. Lim, M. S. Shoichet, Biomaterials 2005, 26, 7436.
[87] P. Gentile, V. Chiono, I. Carmagnola, P. V. Hatton, International journal of molecular sciences 2014, 15, 3640.
[88] A. J. Lasprilla, G. A. Martinez, B. H. Lunelli, A. L. Jardini, R. Maciel Filho, Biotechnol. Adv. 2012, 30, 321.
[89] Z. Sheikh, S. Najeeb, Z. Khurshid, V. Verma, H. Rashid, M. Glogauer, Materials 2015, 8, 5744.
[90] H. K. Makadia, S. J. Siegel, Polymers 2011, 3, 1377.
[91] F. Asghari, M. Samiei, K. Adibkia, A. Akbarzadeh, S. Davaran, Artificial cells, nanomedicine, and biotechnology 2017, 45, 185.
[92] E. Z. Khvalevsky, R. Gabai, I. H. Rachmut, E. Horwitz, Z. Brunschwig, A. Orbach, A. Shemi, T. Golan, A. J. Domb, E. Yavin, Proceedings of the National Academy of Sciences 2013, 110, 20723.
[93] T. Golan, E. Z. Khvalevsky, A. Hubert, R. M. Gabai, N. Hen, A. Segal, A. Domb, G. Harari, E. B. David, S. Raskin, Oncotarget 2015, 6, 24560.
[94] B. D. Weinberg, H. Ai, E. Blanco, J. M. Anderson, J. Gao, Journal of Biomedical Materials Research Part A 2007, 81, 161.
[95] M. A. Woodruff, D. W. Hutmacher, Progress in Polymer Science 2010, 35, 1217.
[96] M. Abedalwafa, F. Wang, L. Wang, C. Li, Rev. Adv. Mater. Sci 2013, 34, 123.
[97] T. K. Dash, V. B. Konkimalla, J. Controlled Release 2012, 158, 15.

[98] W. Chen, Z. Wu, H. Yang, S. Guo, D. Li, L. Cheng, Pharmaceutical development and technology 2014, 19, 223.
[99] H. Brem, P. Gabikian, J. Controlled Release 2001, 74, 63.
[100] R. Cristescu, C. Cojanu, A. Popescu, S. Grigorescu, C. Nastase, F. Nastase, A. Doraiswamy, R. Narayan, I. Stamatin, I. Mihailescu, Appl. Surf. Sci. 2007, 254, 1169.
[101] A. B. Fleming, W. M. Saltzman, Clinical pharmacokinetics 2002, 41, 403.
[102] K. A. Walter, M. A. Cahan, A. Gur, B. Tyler, J. Hilton, O. M. Colvin, P. C. Burger, A. Domb, H. Brem, Cancer research 1994, 54, 2207.
[103] L. K. Fung, M. G. Ewend, A. Sills, E. P. Sipos, R. Thompson, M. Watts, O. M. Colvin, H. Brem, W. M. Saltzman, Cancer Research 1998, 58, 672.
[104] M. S. LESNIAK, U. UPADHYAY, R. GOODWIN, B. TYLER, H. BREM, Anticancer Res. 2005, 25, 3825.
[105] R. T. Wicks, J. Azadi, A. Mangraviti, I. Zhang, L. Hwang, A. Joshi, H. Bow, M. Hutt-Cabezas, K. L. Martin, M. A. Rudek, Neuro-oncology 2014, 17, 70.
[106] M. Westphal, Z. Ram, V. Riddle, D. Hilt, E. Bortey, Acta neurochirurgica 2006, 148, 269.
[107] S. Valtonen, U. l. Timonen, P. Toivanen, H. Kalimo, L. Kivipelto, O. Heiskanen, G. Unsgaard, T. Kuurne, Neurosurgery 1997, 41, 44.
[108] M. Westphal, D. C. Hilt, E. Bortey, P. Delavault, R. Olivares, P. C. Warnke, I. R. Whittle, J. Jääskeläinen, Z. Ram, Neuro-oncology 2003, 5, 79.
[109] H. Brem, S. Piantadosi, P. C. Burger, M. Walker, R. Selker, N. A. Vick, K. Black, M. Sisti, S. Brem, G. Mohr, The Lancet 1995, 345, 1008.
[110]
[111] S. A. Chowdhary, T. Ryken, H. B. Newton, Journal of neuro-oncology 2015, 122, 367.
[112] S. T. Yohe, Y. L. Colson, M. W. Grinstaff, J. Am. Chem. Soc. 2012, 134, 2016.
[113] J. B. Wolinsky, S. T. Yohe, Y. L. Colson, M. W. Grinstaff, Biomacromolecules 2012, 13, 406.
[114] J. B. Wolinsky, R. Liu, J. Walpole, L. R. Chirieac, Y. L. Colson, M. W. Grinstaff, J. Controlled Release 2010, 144, 280.
[115] J. F. Mano, Adv. Eng. Mater. 2008, 10, 515.
[116] L. Klouda, A. G. Mikos, European Journal of Pharmaceutics and Biopharmaceutics 2008, 68, 34.
[117] B. Jeong, S. W. Kim, Y. H. Bae, Advanced Drug Delivery Reviews 2012, 64, 154.
[118] M. A. Ward, T. K. Georgiou, Polymers 2011, 3, 1215.
[119] Y. Qu, B. Y. Chu, J. R. Peng, J. F. Liao, T. T. Qi, K. Shi, X. N. Zhang, Y. Q. Wei, Z. Y. Qian, NPG Asia Materials 2015, 7, e207.
[120] J. Y. Cherng, T. Y. Hou, M. F. Shih, H. Talsma, W. E. Hennink, Int. J. Pharm. 2013, 450, 145.
[121] J. W. Lee, S.-G. Yang, K. Na, Int. J. Pharm. 2012, 427, 276.
[122] N. Genina, J. Holländer, H. Jukarainen, E. Mäkilä, J. Salonen, N. Sandler, European Journal of Pharmaceutical Sciences 2016, 90, 53.
[123] Q.-h. Guo, S.-r. Guo, Z.-m. Wang, Int. J. Pharm. 2007, 333, 95.
[124] J. Liu, Z. Wang, K. Wu, J. Li, W. Chen, Y. Shen, S. Guo, Biomaterials 2015, 53, 592.
[125] D. Liang, B. S. Hsiao, B. Chu, Advanced drug delivery reviews 2007, 59, 1392.
[126] N. Annabi, A. Tamayol, J. A. Uquillas, M. Akbari, L. E. Bertassoni, C. Cha, G. Camci‐Unal, M. R. Dokmeci, N. A. Peppas, A. Khademhosseini, Adv. Mater. 2014, 26, 85.
[127] R. D. Pedde, B. Mirani, A. Navaei, T. Styan, S. Wong, M. Mehrali, A. Thakur, N. K. Mohtaram, A. Bayati, A. Dolatshahi‐Pirouz, Adv. Mater. 2017.
[128] A. Balaji, M. Vellayappan, A. John, A. Subramanian, S. Jaganathan, E. Supriyanto, S. Razak, RSC Advances 2015, 5, 57984.

[129] A. Repanas, S. Andriopoulou, B. Glasmacher, Journal of Drug Delivery Science and Technology 2016, 31, 137.
[130] A. Rogina, Appl. Surf. Sci. 2014, 296, 221.
[131] X. Hu, S. Liu, G. Zhou, Y. Huang, Z. Xie, X. Jing, J. Controlled Release 2014, 185, 12.
[132] A. J. Meinel, O. Germershaus, T. Luhmann, H. P. Merkle, L. Meinel, European Journal of Pharmaceutics and Biopharmaceutics 2012, 81, 1.
[133] Y. Lu, J. Huang, G. Yu, R. Cardenas, S. Wei, E. K. Wujcik, Z. Guo, Wiley Interdisciplinary Reviews: Nanomedicine and Nanobiotechnology 2016.
[134] Y. J. Son, W. J. Kim, H. S. Yoo, Arch. Pharmacal Res. 2014, 37, 69.
[135] E. Yan, Y. Fan, Z. Sun, J. Gao, X. Hao, S. Pei, C. Wang, L. Sun, D. Zhang, Materials Science and Engineering: C 2014, 41, 217.
[136] D. Han, A. J. Steckl, ACS applied materials & interfaces 2013, 5, 8241.
[137] G.-Z. Yang, J.-J. Li, D.-G. Yu, M.-F. He, J.-H. Yang, G. R. Williams, Acta Biomaterialia 2017, 53, 233.
[138] L. E. Aguilar, A. GhavamiNejad, C. H. Park, C. S. Kim, Nanomedicine: Nanotechnology, Biology and Medicine 2017, 13, 527.
[139] G. Yang, J. Wang, Y. Wang, L. Li, X. Guo, S. Zhou, ACS nano 2015, 9, 1161.
[140] P. X. Ma, Advanced drug delivery reviews 2008, 60, 184.
[141] Z. Chen, Z. Chen, A. Zhang, J. Hu, X. Wang, Z. Yang, Biomaterials science 2016, 4, 922.
[142] R. Casasola, N. L. Thomas, A. Trybala, S. Georgiadou, Polymer 2014, 55, 4728.
[143] T. J. Sill, H. A. von Recum, Biomaterials 2008, 29, 1989.
[144] C. Monterrubio, G. Pascual-Pasto, F. Cano, M. Vila-Ubach, A. Manzanares, P. Schaiquevich, J. A. Tornero, A. Sosnik, J. Mora, A. M. Carcaboso, Biomaterials 2016, 79, 69.
[145] D. Liu, S. Liu, X. Jing, X. Li, W. Li, Y. Huang, Biomaterials 2012, 33, 4362.
[146] G. Li, Y. Chen, J. Hu, X. Wu, J. Hu, X. He, J. Li, Z. Zhao, Z. Chen, Y. Li, Biomaterials 2013, 34, 9451.
[147] J. Zhang, X. Wang, T. Liu, S. Liu, X. Jing, Drug delivery 2016, 23, 784.
[148] S. H. Ranganath, Y. Fu, D. Y. Arifin, I. Kee, L. Zheng, H.-S. Lee, P. K.-H. Chow, C.-H. Wang, Biomaterials 2010, 31, 5199.
[149] Y.-Y. Tseng, Y.-C. Huang, T.-C. Yang, S.-T. Yang, S.-C. Liu, T.-M. Chang, Y.-C. Kau, S.-J. Liu, Scientific reports 2016, 6.
[150] A. Cipitria, A. Skelton, T. Dargaville, P. Dalton, D. Hutmacher, J. Mater. Chem. 2011, 21, 9419.
[151] Y. Chen, Z. Hou, B. Liu, S. Huang, C. Li, J. Lin, Dalton Transactions 2015, 44, 3118.
[152] J. A. Kaplan, R. Liu, J. D. Freedman, R. Padera, J. Schwartz, Y. L. Colson, M. W. Grinstaff, Biomaterials 2016, 76, 273.
[153] Q. P. Pham, U. Sharma, A. G. Mikos, Tissue Eng. 2006, 12, 1197.
[154] S.-Y. Kim, M. Kim, M.-k. Kim, H. Lee, D. K. Lee, D.-H. Lee, S.-G. Yang, Biomed. Microdevices 2014, 16, 897.
[155] J. Norman, R. D. Madurawe, C. M. Moore, M. A. Khan, A. Khairuzzaman, Advanced drug delivery reviews 2017, 108, 39.
[156] B. Stevens, Y. Yang, A. Mohandas, B. Stucker, K. T. Nguyen, Journal of biomedical materials research Part B: applied biomaterials 2008, 85, 573.
[157] S. J. Hollister, Nature materials 2005, 4, 518.
[158] H.-H. G. Song, K. M. Park, S. Gerecht, Advanced Drug Delivery Reviews 2014, 79–80, 19.
[159] L. Gu, D. J. Mooney, Nature Reviews Cancer 2016, 16, 56.
[160] S. Knowlton, S. Onal, C. H. Yu, J. J. Zhao, S. Tasoglu, Trends Biotechnol. 2015, 33, 504.

[161] N. Sandler, M. Preis, Trends in Pharmacological Sciences 2016, 37, 1070.
[162] J. Jang, H.-G. Yi, D.-W. Cho, ACS Biomaterials Science & Engineering 2016, 2, 1722.
[163] C. Bellehumeur, L. Li, Q. Sun, P. Gu, Journal of Manufacturing Processes 2004, 6, 170.
[164] I. Zein, D. W. Hutmacher, K. C. Tan, S. H. Teoh, Biomaterials 2002, 23, 1169.
[165] D. M. Kirchmajer, R. Gorkin III, Journal of Materials Chemistry B 2015, 3, 4105.
[166] W. Zhu, X. Ma, M. Gou, D. Mei, K. Zhang, S. Chen, Curr. Opin. Biotechnol. 2016, 40, 103.
[167] A. V. Do, B. Khorsand, S. M. Geary, A. K. Salem, Advanced healthcare materials 2015, 4, 1742.
[168] P. Agarwal, I. D. Rupenthal, Drug Discovery Today 2013, 18, 337.
[169] A. Hatefi, B. Amsden, J. Controlled Release 2002, 80, 9.
[170] A. Fakhari, J. Anand Subramony, J. Controlled Release 2015, 220, 465.
[171] S. Wang, Y. Chen, X. Li, W. Gao, L. Zhang, J. Liu, Y. Zheng, H. Chen, J. Shi, Advanced Materials 2015, 27, 7117.
[172] Y. Chen, L. Jiang, R. Wang, M. Lu, Q. Zhang, Y. Zhou, Z. Wang, G. Lu, P. Liang, H. Ran, Adv. Mater. 2014, 26, 7468.
[173] C.-W. Hsiao, E.-Y. Chuang, H.-L. Chen, D. Wan, C. Korupalli, Z.-X. Liao, Y.-L. Chiu, W.-T. Chia, K.-J. Lin, H.-W. Sung, Biomaterials 2015, 56, 26.
[174] J. Shi, W. Guobao, H. Chen, W. Zhong, X. Qiu, M. M. Xing, Polymer Chemistry 2014, 5, 6180.
[175] J. Liu, C. Qi, K. Tao, J. Zhang, J. Zhang, L. Xu, X. Jiang, Y. Zhang, L. Huang, Q. Li, ACS applied materials & interfaces 2016, 8, 6411.
[176] T. Fourniols, L. D. Randolph, A. Staub, K. Vanvarenberg, J. G. Leprince, V. Préat, A. des Rieux, F. Danhier, J. Controlled Release 2015, 210, 95.
[177] X. Wang, C. Wang, X. Wang, Y. Wang, Q. Zhang, Y. Cheng, Chem. Mater. 2017.
[178] J. D. Kretlow, L. Klouda, A. G. Mikos, Advanced drug delivery reviews 2007, 59, 263.
[179] A. Gutowska, B. Jeong, M. Jasionowski, The Anatomical Record 2001, 263, 342.
[180] L. Yu, J. Ding, Chem. Soc. Rev. 2008, 37, 1473.
[181] M. Norouzi, B. Nazari, D. W. Miller, Drug Discovery Today 2016, 21, 1835.
[182] J. Zhu, Biomaterials 2010, 31, 4639.
[183] S. Zalipsky, Bioconjugate Chem. 1995, 6, 150.
[184] H. Tan, K. G. Marra, Materials 2010, 3, 1746.
[185] H. W. Seo, D. Y. Kwon, J. S. Kwon, L. M. Jin, B. Lee, J. H. Kim, B. H. Min, M. S. Kim, Biomaterials 2013, 34, 2748.
[186] V. G. Phan, E. Lee, J. H. Maeng, T. Thambi, B. S. Kim, D. Lee, D. S. Lee, RSC Advances 2016, 6, 41644.
[187] A. A. Ghahremankhani, F. Dorkoosh, R. Dinarvand, Pharmaceutical development and technology 2008, 13, 49.
[188] K. Nagahama, D. Kawano, N. Oyama, A. Takemoto, T. Kumano, J. Kawakami, Biomacromolecules 2015, 16, 880.
[189] H. Ma, C. He, Y. Cheng, Z. Yang, J. Zang, J. Liu, X. Chen, ACS applied materials & interfaces 2015, 7, 27040.
[190] L. Yu, T. Ci, S. Zhou, W. Zeng, J. Ding, Biomaterials Science 2013, 1, 411.
[191] Y. Zhang, J. Ding, D. Sun, H. Sun, X. Zhuang, F. Chang, J. Wang, X. Chen, Materials Science and Engineering: C 2015, 49, 262.
[192] C. A. Bagley, M. J. Bookland, J. A. Pindrik, T. Ozmen, Z. L. Gokaslan, T. F. Witham, 2007.

[193] G. M. Zentner, R. Rathi, C. Shih, J. C. McRea, M.-H. Seo, H. Oh, B. Rhee, J. Mestecky, Z. Moldoveanu, M. Morgan, J. Controlled Release 2001, 72, 203.
[194] K. Matthes, M. Mino-Kenudson, D. V. Sahani, N. Holalkere, K. D. Fowers, R. Rathi, W. R. Brugge, Gastrointestinal endoscopy 2007, 65, 448.
[195] S. J. Vukelja, S. P. Anthony, J. C. Arseneau, B. S. Berman, C. C. Cunningham, J. J. Nemunaitis, W. E. Samlowski, K. D. Fowers, Anti-cancer drugs 2007, 18, 283.
[196] N. L. Elstad, K. D. Fowers, Advanced Drug Delivery Reviews 2009, 61, 785.
[197] Y. Wang, C. Gong, L. Yang, Q. Wu, S. Shi, H. Shi, Z. Qian, Y. Wei, BMC cancer 2010, 10, 402.
[198] X. Wu, Y. Wu, H. Ye, S. Yu, C. He, X. Chen, J. Controlled Release 2017, 255, 81.
[199] Y. Cheng, C. He, J. Ding, C. Xiao, X. Zhuang, X. Chen, Biomaterials 2013, 34, 10338.
[200] E. Bakaic, N. M. Smeets, T. Hoare, RSC Advances 2015, 5, 35469.
[201] H. Zhang, X. Zhu, Y. Ji, X. Jiao, Q. Chen, L. Hou, H. Zhang, Z. Zhang, Journal of Materials Chemistry B 2015, 3, 6310.
[202] X. Li, R. Fan, Y. Wang, M. Wu, A. Tong, J. Shi, M. Xiang, L. Zhou, G. Guo, RSC Advances 2015, 5, 101494.
[203] X. Zhu, Y. Zhang, H. Huang, H. Zhang, L. Hou, Z. Zhang, J. Biomater. Appl. 2016, 30, 1230.
[204] L. Zhao, L. Zhu, F. Liu, C. Liu, Q. Wang, C. Zhang, J. Li, J. Liu, X. Qu, Z. Yang, Int. J. Pharm. 2011, 410, 83.
[205] D. S. Shaker, M. A. Shaker, A. Klingner, M. S. Hanafy, Journal of Drug Delivery Science and Technology 2016, 35, 155.
[206] Y. Mao, X. Li, G. Chen, S. Wang, J. Pharm. Sci. 2015.
[207] R. Fan, A. Tong, X. Li, X. Gao, L. Mei, L. Zhou, X. Zhang, C. You, G. Guo, International journal of nanomedicine 2015, 10, 7291.
[208] L. Gao, X. Wang, J. Ma, D. Hao, P. Wei, L. Zhou, G. Liu, Colloids and Surfaces B: Biointerfaces 2016, 140, 307.
[209] D. Y. Kim, D. Y. Kwon, J. S. Kwon, J. H. Park, S. H. Park, H. J. Oh, J. H. Kim, B. H. Min, K. Park, M. S. Kim, Biomaterials 2016, 85, 232.
[210] N. U. Khaliq, K. S. Oh, F. C. Sandra, Y. Joo, J. Lee, Y. Byun, I.-S. Kim, I. C. Kwon, J. H. Seo, S. Y. Kim, S. H. Yuk, J. Controlled Release 2017, 255, 258.
[211] H. Hu, Z. Lin, B. He, W. Dai, X. Wang, J. Wang, X. Zhang, H. Zhang, Q. Zhang, J. Controlled Release 2015, 220, 189.
[212] N. Zhang, X. Xu, X. Zhang, D. Qu, L. Xue, R. Mo, C. Zhang, Int. J. Pharm. 2016, 497, 210.
[213] M.-T. Sheu, H.-J. Jhan, C.-Y. Su, L.-C. Chen, C.-E. Chang, D.-Z. Liu, H.-O. Ho, Colloids and Surfaces B: Biointerfaces 2016, 143, 260.
[214] T. Li, M. Zhang, J. Wang, T. Wang, Y. Yao, X. Zhang, C. Zhang, N. Zhang, The AAPS journal 2016, 18, 146.
[215] Z. Liu, G. Xu, C. Wang, C. Li, P. Yao, Int. J. Pharm. 2017, 530, 53.
[216] D.-D. Guo, S.-H. Hong, H.-L. Jiang, J.-H. Kim, A. Minai-Tehrani, J.-E. Kim, J.-Y. Shin, T. Jiang, Y.-K. Kim, Y.-J. Choi, Biomaterials 2012, 33, 2272.
[217] M. Guvendiren, H. D. Lu, J. A. Burdick, Soft matter 2012, 8, 260.
[218] M. Patenaude, T. Hoare, ACS Macro Letters 2012, 1, 409.
[219] M. Zhou, S. Liu, Y. Jiang, H. Ma, M. Shi, Q. Wang, W. Zhong, W. Liao, M. M. Xing, Adv. Funct. Mater. 2015, 25, 4730.
[220] X. Xu, Z. Huang, Z. Huang, X. Zhang, S. He, X. Sun, Y. Shen, M. Yan, C. Zhao, ACS Applied Materials & Interfaces 2017.
[221] H. Zhao, J. Xu, J. Wan, S. Geng, H. Li, X. Peng, Q. Fu, M. He, Y. Zhao, X. Yang, Nanoscale 2017, 9, 5859.

[222] S. Pina, J. M. Oliveira, R. L. Reis, Adv. Mater. 2015, 27, 1143.
[223] R. Xing, K. Liu, T. Jiao, N. Zhang, K. Ma, R. Zhang, Q. Zou, G. Ma, X. Yan, Adv. Mater. 2016, 28, 3669.
[224] C. Kojima, T. Suehiro, K. Watanabe, M. Ogawa, A. Fukuhara, E. Nishisaka, A. Harada, K. Kono, T. Inui, Y. Magata, Acta biomaterialia 2013, 9, 5673.
[225] H. Peng, H. Yang, L. Song, Z. Zhou, J. Sun, Y. Du, K. Lu, T. Li, A. Yin, J. Xu, Journal of Experimental & Clinical Cancer Research 2016, 35, 57.
[226] S. P. Monga, R. Wadleigh, A. Sharma, H. Adib, D. Strader, G. Singh, J. W. Harmon, M. Berlin, D. K. Monga, L. Mishra, American journal of clinical oncology 2000, 23, 386.
[227] A. H. Burris III, C. L. Vogel, D. Castro, L. Mishra, M. Schwarz, S. Spencer, D. D. Oakes, A. Korey, E. K. Orenberg, Otolaryngology—Head and Neck Surgery 1998, 118, 496.
[228] B. L. Wenig, J. A. Werner, D. J. Castro, K. S. Sridhar, H. S. Garewal, W. Kehrl, A. Pluzanska, O. Arndt, P. D. Costantino, G. M. Mills, Archives of Otolaryngology–Head & Neck Surgery 2002, 128, 880.
[229] T. W. Leung, S. Yu, P. Johnson, J. Geschwind, T. Vogl, K. Engelmann, G. J. Gores, M. Giovannini, J. O'grady, M. Heneghan, Journal of clinical oncology 2003, 21, 652.
[230] J. Berger, M. Reist, J. M. Mayer, O. Felt, N. A. Peppas, R. Gurny, European Journal of Pharmaceutics and Biopharmaceutics 2004, 57, 19.
[231] N. Bhattarai, J. Gunn, M. Zhang, Advanced Drug Delivery Reviews 2010, 62, 83.
[232] E. Ruel-Gariépy, J.-C. Leroux, European Journal of Pharmaceutics and Biopharmaceutics 2004, 58, 409.
[233] S. Ren, Y. Dai, C. Li, Z. Qiu, X. Wang, F. Tian, S. Zhou, Q. Liu, H. Xing, Y. Lu, European Journal of Pharmaceutical Sciences 2016, 92, 137.
[234] G. Tripodo, A. Trapani, M. L. Torre, G. Giammona, G. Trapani, D. Mandracchia, European Journal of Pharmaceutics and Biopharmaceutics 2015, 97, 400.
[235] H. Tan, C. M. Ramirez, N. Miljkovic, H. Li, J. P. Rubin, K. G. Marra, Biomaterials 2009, 30, 6844.
[236] G. Bajaj, M. R. Kim, S. I. Mohammed, Y. Yeo, J. Controlled Release 2012, 158, 386.
[237] K. Ueda, J. Akiba, S. Ogasawara, K. Todoroki, M. Nakayama, A. Sumi, H. Kusano, S. Sanada, S. Suekane, K. Xu, Acta biomaterialia 2016, 29, 103.
[238] K. Xu, F. Lee, S. J. Gao, J. E. Chung, H. Yano, M. Kurisawa, J. Controlled Release 2013, 166, 203.
[239] S. Doppalapudi, A. Jain, A. J. Domb, W. Khan, Expert opinion on drug delivery 2016, 13, 891.
[240] S. J. Bidarra, C. C. Barrias, P. L. Granja, Acta Biomaterialia 2014, 10, 1646.
[241] I. Teasdale, S. Wilfert, I. Nischang, O. Brüggemann, Polymer Chemistry 2011, 2, 828.
[242] I. Teasdale, O. Brüggemann, Polymers 2013, 5, 161.
[243] A. M. Al-Abd, K.-Y. Hong, S.-C. Song, H.-J. Kuh, J. Controlled Release 2010, 142, 101.
[244] Z.-Q. Zhang, S.-C. Song, Biomaterials 2017, 132, 16.
[245] J. Wang, D. Wang, H. Yan, L. Tao, Y. Wei, Y. Li, X. Wang, W. Zhao, Y. Zhang, L. Zhao, Journal of Materials Chemistry B 2017, 5, 4110.
[246] L. Yang, Y. Li, Y. Gou, X. Wang, X. Zhao, L. Tao, Polymer Chemistry 2017.
[247] N. Huebsch, C. J. Kearney, X. Zhao, J. Kim, C. A. Cezar, Z. Suo, D. J. Mooney, Proceedings of the National Academy of Sciences 2014, 111, 9762.
[248] J. Hu, Y. Chen, Y. Li, Z. Zhou, Y. Cheng, Biomaterials 2017, 112, 133.
[249] X. Wang, C. Wang, Q. Zhang, Y. Cheng, Chemical Communications 2016, 52, 978.
[250] D. L. Taylor, Adv. Mater. 2016.
[251] R. A. Siegel, M. J. Rathbone, in *Fundamentals and Applications of Controlled Release Drug Delivery*, Springer, 2012, 19.

[252] R. Alford, H. M. Simpson, J. Duberman, G. C. Hill, M. Ogawa, C. Regino, H. Kobayashi, P. L. Choyke, Molecular imaging 2009, 8, 7290.2009. 00031.
[253] Z. Wang, Y. Zhang, J. Zhang, L. Huang, J. Liu, Y. Li, G. Zhang, S. C. Kundu, L. Wang, Scientific reports 2014, 4.
[254] D. Schmaljohann, Advanced Drug Delivery Reviews 2006, 58, 1655.
[255] D. A. LaVan, T. McGuire, R. Langer, Nat. Biotechnol. 2003, 21, 1184.
[256] R. Farra, N. F. Sheppard, L. McCabe, R. M. Neer, J. M. Anderson, J. T. Santini, M. J. Cima, R. Langer, Science translational medicine 2012, 4, 122ra21.
[257] R. C. Coombes, Science translational medicine 2015, 7, 284ps10.
[258] P. Dario, M. C. Carrozza, A. Benvenuto, A. Menciassi, Journal of Micromechanics and Microengineering 2000, 10, 235.
[259] O. Jonas, H. M. Landry, J. E. Fuller, J. T. Santini, J. Baselga, R. I. Tepper, M. J. Cima, R. Langer, Science translational medicine 2015, 7, 284ra57.
[260] P. Song, D. J. H. Tng, R. Hu, G. Lin, E. Meng, K. T. Yong, Advanced healthcare materials 2013, 2, 1170.
[261] A. Shademani, H. Zhang, J. K. Jackson, M. Chiao, Adv. Funct. Mater. 2017, 27.
[262] S. R. Paul, S. K. Nayak, A. Anis, K. Pal, Polymer-Plastics Technology and Engineering 2016, 55, 965.
[263] A. R. Grayson, R. S. Shawgo, A. M. Johnson, N. T. Flynn, Y. Li, M. J. Cima, R. Langer, Proceedings of the IEEE 2004, 92, 6.
[264] A. C. R. Grayson, R. S. Shawgo, Y. Li, M. J. Cima, Advanced drug delivery reviews 2004, 56, 173.
[265] B. C. Masi, B. M. Tyler, H. Bow, R. T. Wicks, Y. Xue, H. Brem, R. Langer, M. J. Cima, Biomaterials 2012, 33, 5768.
[266] A. Cobo, R. Sheybani, E. Meng, Advanced healthcare materials 2015, 4, 969.
[267] H. Gensler, R. Sheybani, P.-Y. Li, R. Lo, S. Zhu, K.-T. Yong, I. Roy, P. N. Prasad, R. Masood, U. K. Sinha, "Implantable MEMS drug delivery device for cancer radiation reduction", presented at *Micro Electro Mechanical Systems (MEMS), 2010 IEEE 23rd International Conference on*, 2010.
[268] S. Y. Chin, Y. C. Poh, A.-C. Kohler, J. T. Compton, L. L. Hsu, K. M. Lau, S. Kim, B. W. Lee, F. Y. Lee, S. K. Sia, Science Robotics 2017, 2, eaah6451.
[269] A. S. Cheung, D. J. Mooney, Nano today 2015, 10, 511.
[270] W. J. Lesterhuis, J. B. Haanen, C. J. Punt, Nature reviews. Drug discovery 2011, 10, 591.
[271] S. H. van der Burg, R. Arens, F. Ossendorp, T. van Hall, C. J. Melief, Nature Reviews Cancer 2016, 16, 219.
[272] N. Oliva, J. o. Conde, K. Wang, N. Artzi, Acc. Chem. Res. 2017.
[273] S. T. Koshy, D. J. Mooney, Curr. Opin. Biotechnol. 2016, 40, 1.
[274] C. Wang, Y. Ye, Q. Hu, A. Bellotti, Z. Gu, Adv. Mater. 2017.
[275] S. A. Bencherif, R. W. Sands, O. A. Ali, W. A. Li, S. A. Lewin, T. M. Braschler, T.-Y. Shih, C. S. Verbeke, D. Bhatta, G. Dranoff, Nature communications 2015, 6.
[276] S. A. Rosenberg, N. P. Restifo, Science 2015, 348, 62.
[277] S. A. Rosenberg, N. P. Restifo, J. C. Yang, R. A. Morgan, M. E. Dudley, Nature reviews. Cancer 2008, 8, 299.
[278] A. Monette, C. Ceccaldi, E. Assaad, S. Lerouge, R. Lapointe, Biomaterials 2016, 75, 237.
[279] R. Aliperta, P. B. Welzel, R. Bergmann, U. Freudenberg, N. Berndt, A. Feldmann, C. Arndt, S. Koristka, M. Stanzione, M. Cartellieri, Scientific Reports 2017, 7, 42855.

Figure captions:

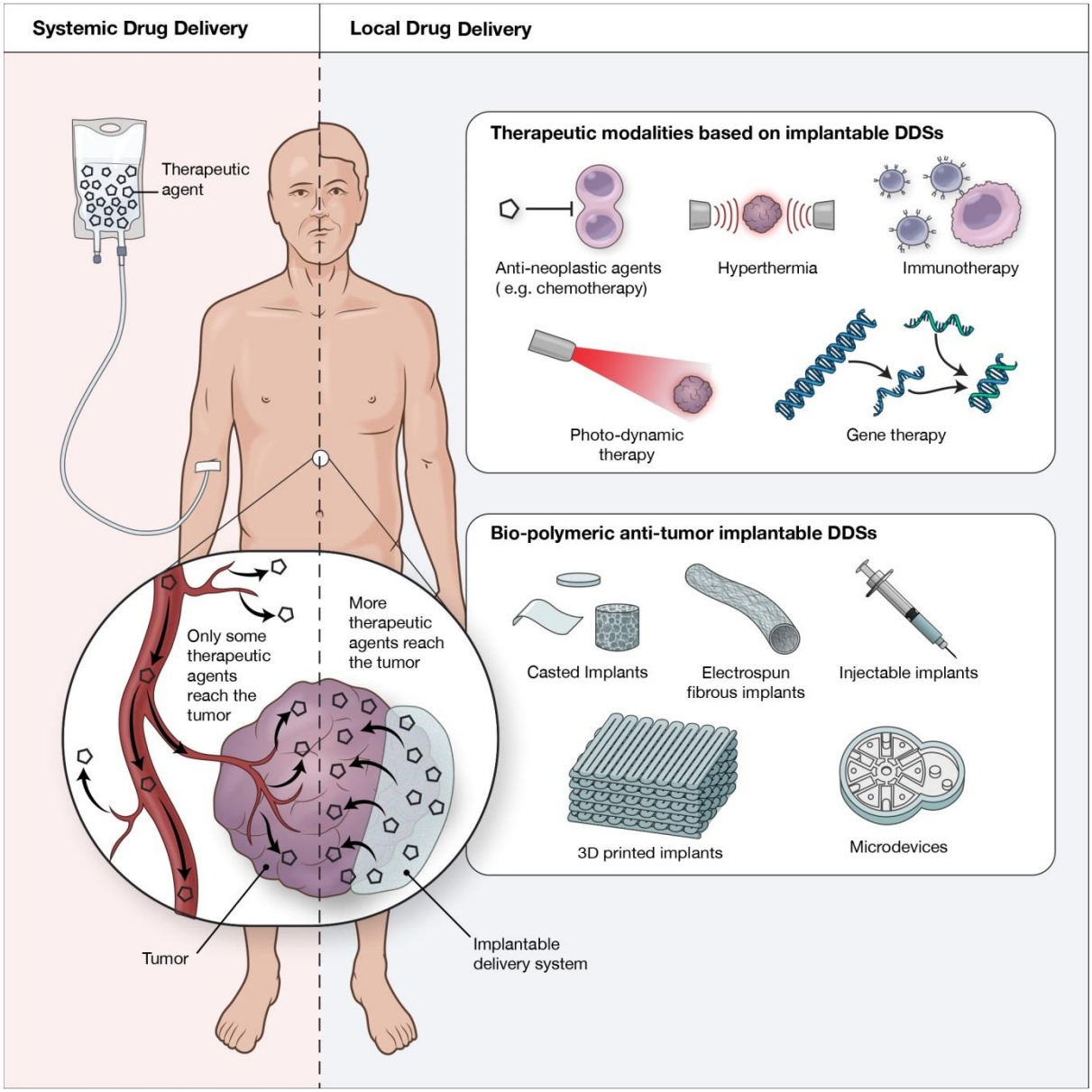

Figure 1. Schematic of systemic drug delivery versus local drug delivery for treatment of malignant tumors, including various types of bio-polymeric implantable systems used for local drug delivery and different anti-cancer therapeutic modalities employed based on these implantable systems.

\

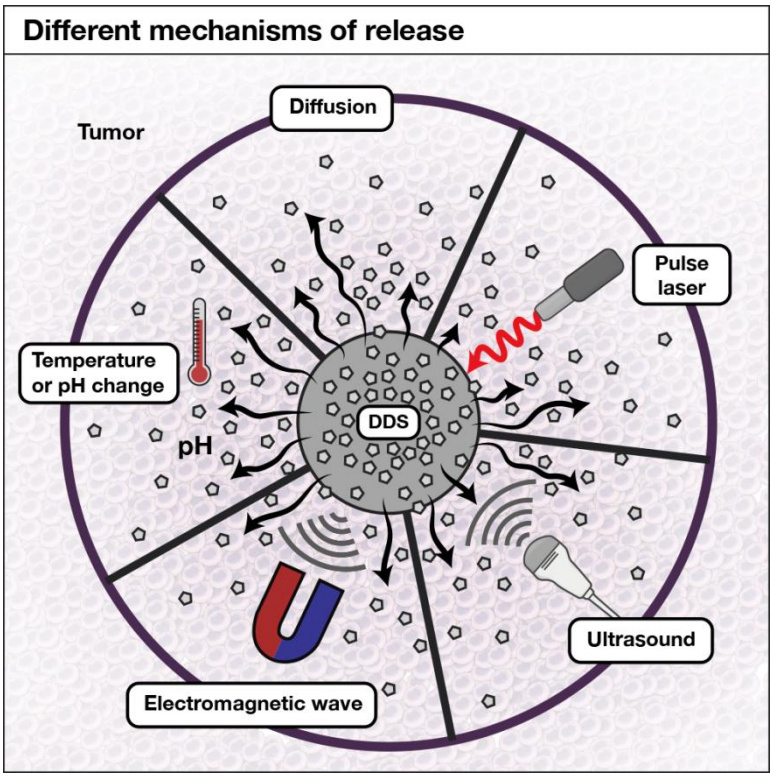

Figure 2. Schematic showing different mechanisms of drug release from bio-polymeric implantable drug delivery systems (DDSs).

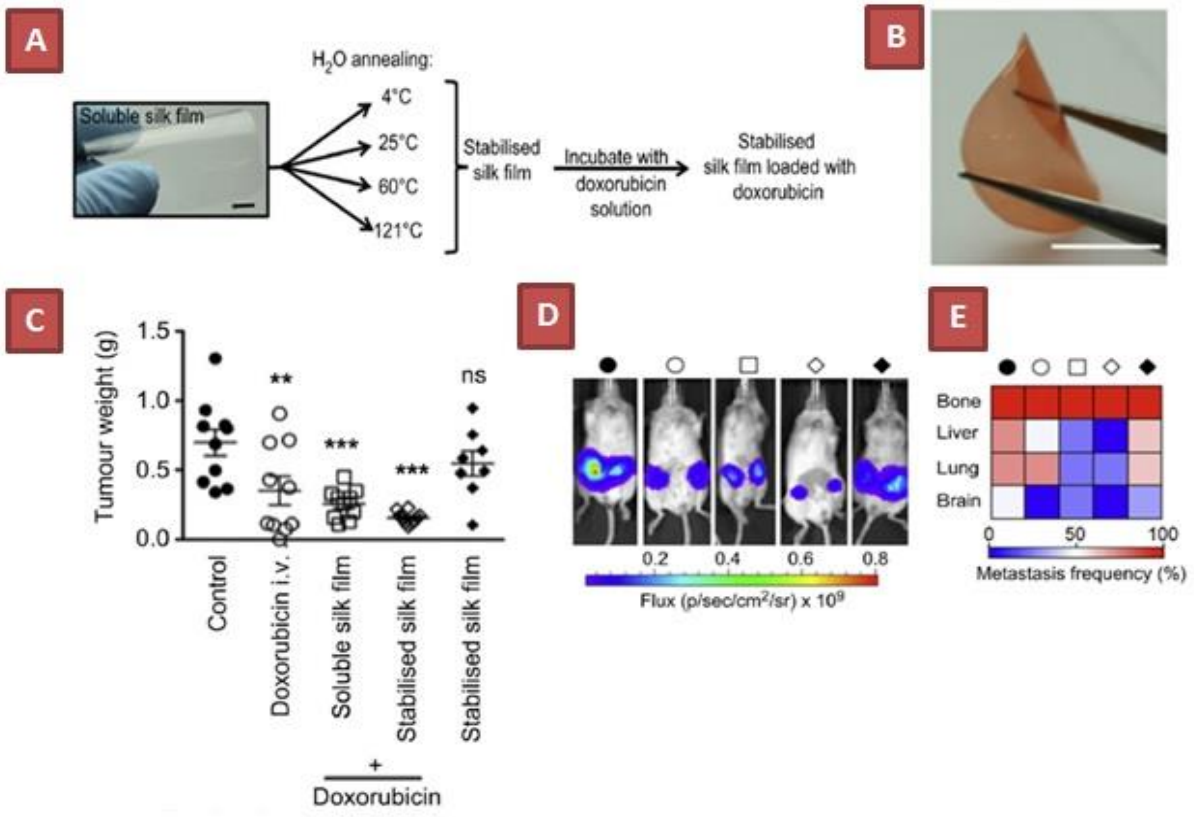

Figure 3. Preparation and *in vivo* anti-tumor performance of DOX loaded films. A) Strategies to generate doxorubicin-loaded films that are water-insoluble with variable β-sheet content. B) Free-standing doxorubicin-loaded silk films in the dry state. C) Weight of primary tumours at the end of the study (week 6). D) *In vivo* tumor cell-specific bioluminescence of representative mice from each treatment group at week 6. Plot symbols are defined in panel (C). E) Metastatic spread of cancer cells to organs at week 6. Plot symbols are defined in panel (C), Reprinted from [21], Copyright (2012), with permission from Elsevier.

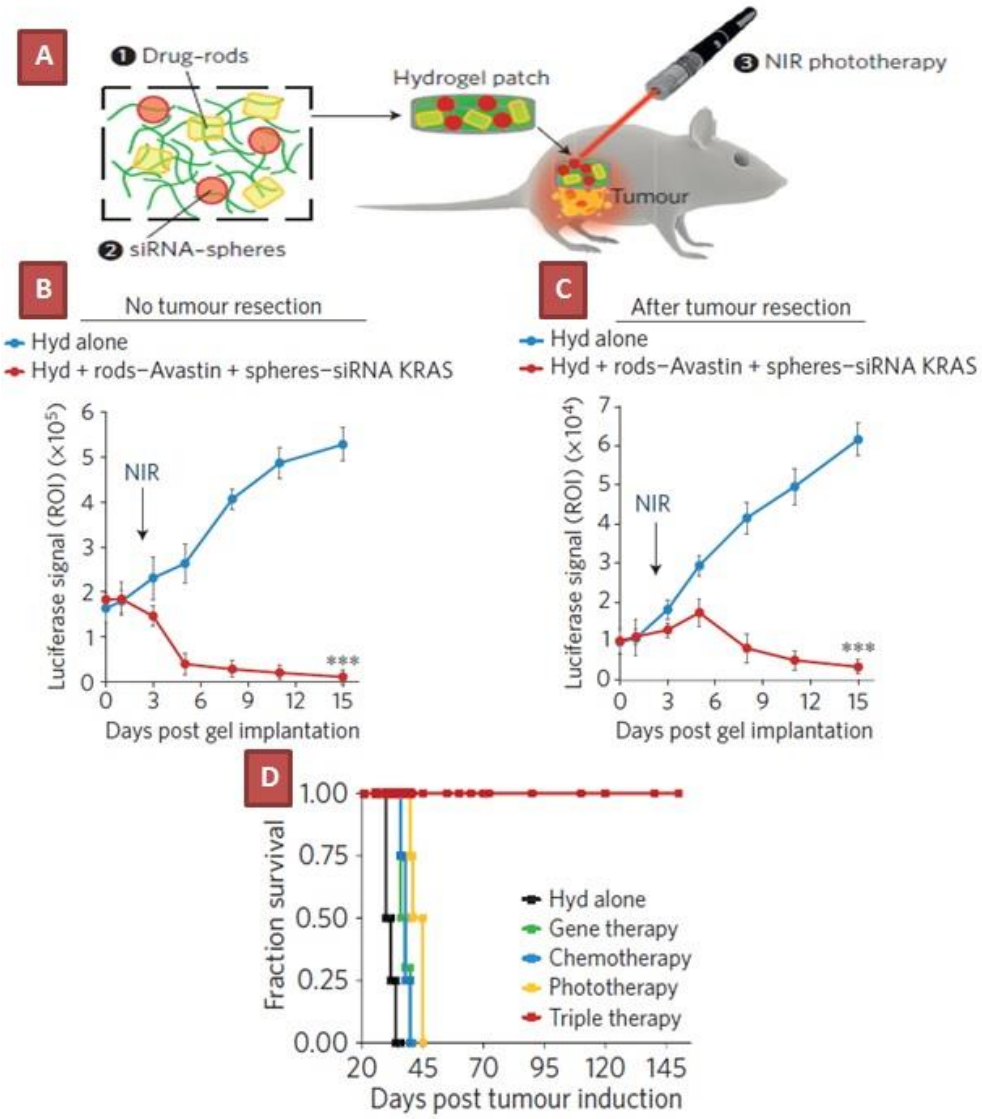

Figure 4. Dextran-based hydrogel scaffold as prophylactic agent for *in vivo* local gene/drug delivery combined with phototherapy, before and after tumor resection in mice model of colorectal cancer. A) Development of smart hydrogel-nanoparticle patch and subsequent implantation in mice model. B) Tumor burden following treatment as measured by luciferase activity, without tumor resection, C) and after tumor resection. D) Survival plot analysis of mice treated with hydrogel scaffolds for single therapies or triple therapy. Reprinted by permission from Macmillan Publishers Ltd: Nature Materials [67], Copyright (2016).

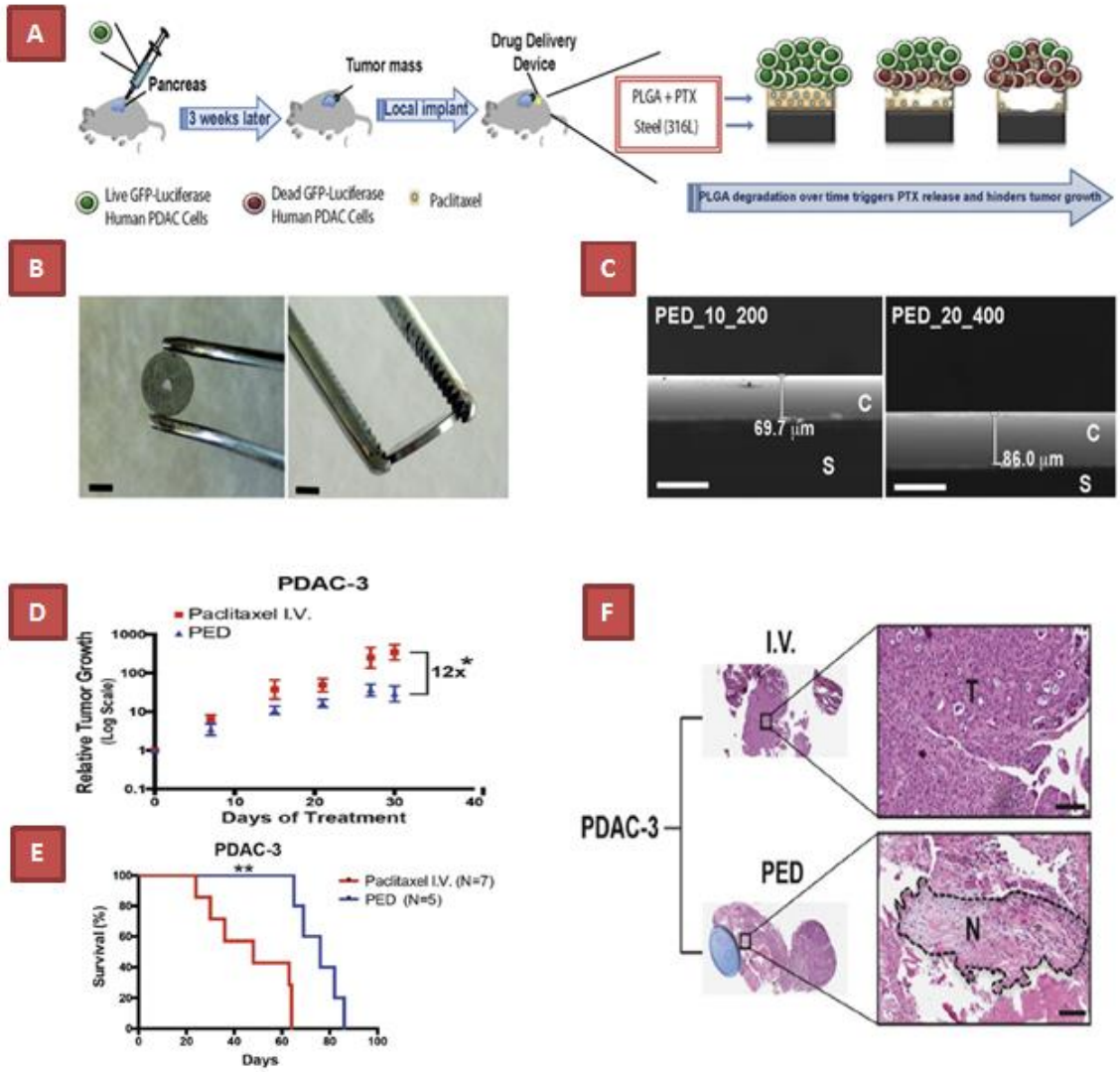

Figure 5. Design, characterization and *in vivo* anti-tumor performance of implantable paclitaxel eluting device (PED). A) Schematic of localized therapeutic approach with PED. B) Macroscopic visualizations of the local delivery device. C) Scanning electron microscopy images of PLGA coating on top of steel ("C" = coating and "S" = steel). D) Relative tumor growth curves of PDAC-3 mouse xenografts after treatment with either paclitaxel intravenous or PED treatment. E) Survival plot showing longer median overall survival (28 day increase) for mice treated with PED compared to mice treated with I.V. injection of paclitaxel. F) Histological analysis of PDAC-3 tumors after treatment with PED showing higher areas of necrosis (N) compared to preserved tumor structure (T) in group treated with I.V. paclitaxel. Reprinted from [28], Copyright (2016), with permission from Elsevier.

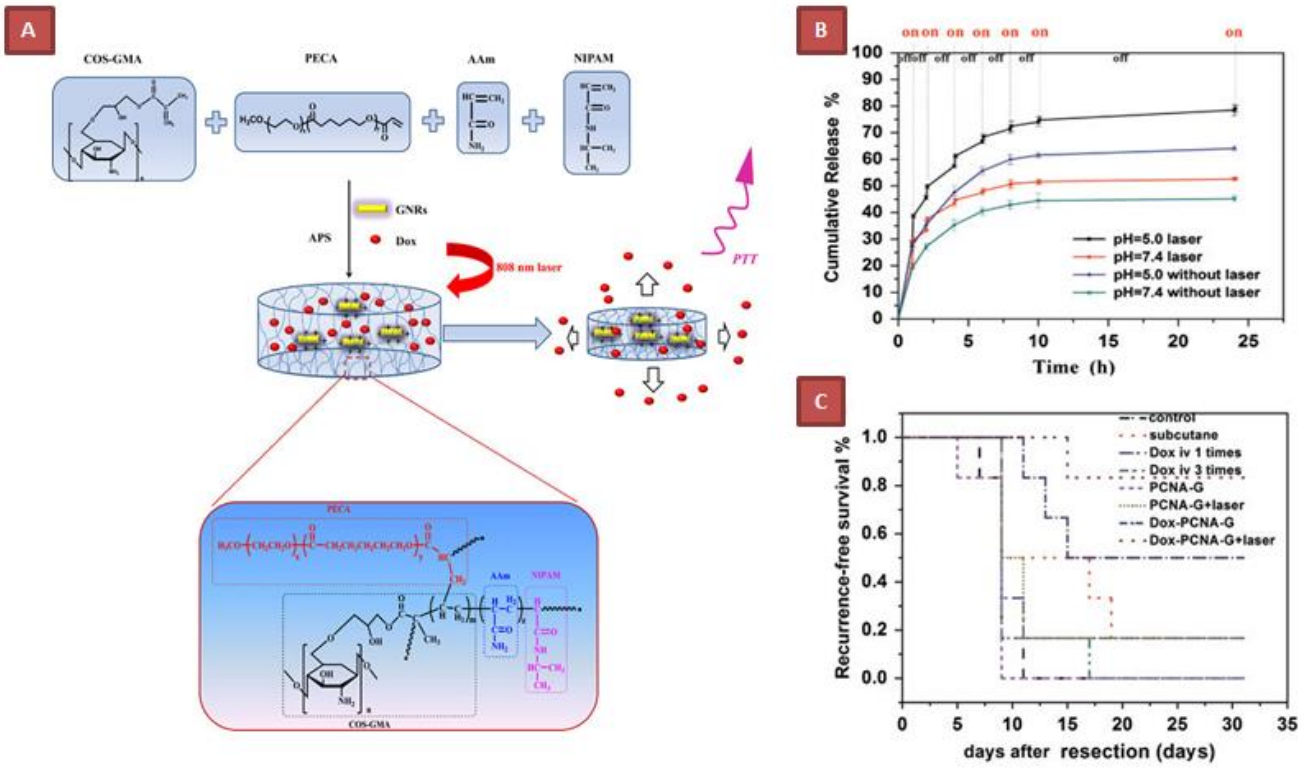

Figure 6. pNIPAAm-based hybrid hydrogel for preventing post-operative recurrence of breast cancer. A) Design of hybrid hydrogel and mechanism of operation of resulting DDS by dual DOX release and photothermal therapy (PTT). B) *In vitro* release profile of DOX from the DDS in PBS. C) *In vivo* locoregional tumor recurrence. Reprinted by permission from Macmillan Publishers Ltd: NPG Asia Materials [119], Copyright (2015).

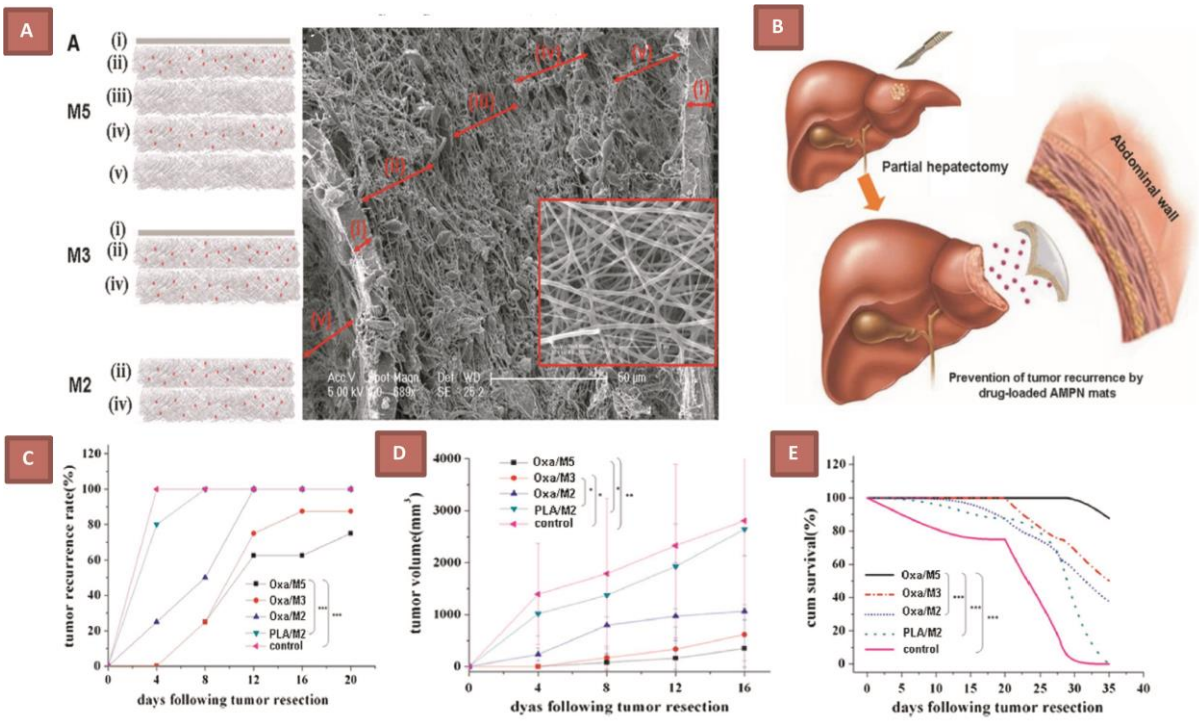

Figure 7. Drug loaded asymmetric multilayer PLA nanofibers (AMPN) for preventing liver cancer recurrence. A) Graphical presentation of multilayer nanofibers and scanning electron microscopy image of five layered (M5) nanofibrous mat. The top layer (i) in M5 and M3 mats contained PLA films to allow one sided release of drugs. B) Schematic illustration of performance of drug-loaded AMPN mats in human body for prevention of tumor recurrence after HCC surgery. C) Tumor recurrence rate, D) average tumor volume, and E) survival time as a function of time, for treated animals, post "subcutaneous tumor" surgery. Reprinted from [39], Copyright (2015), with permission from Elsevier.

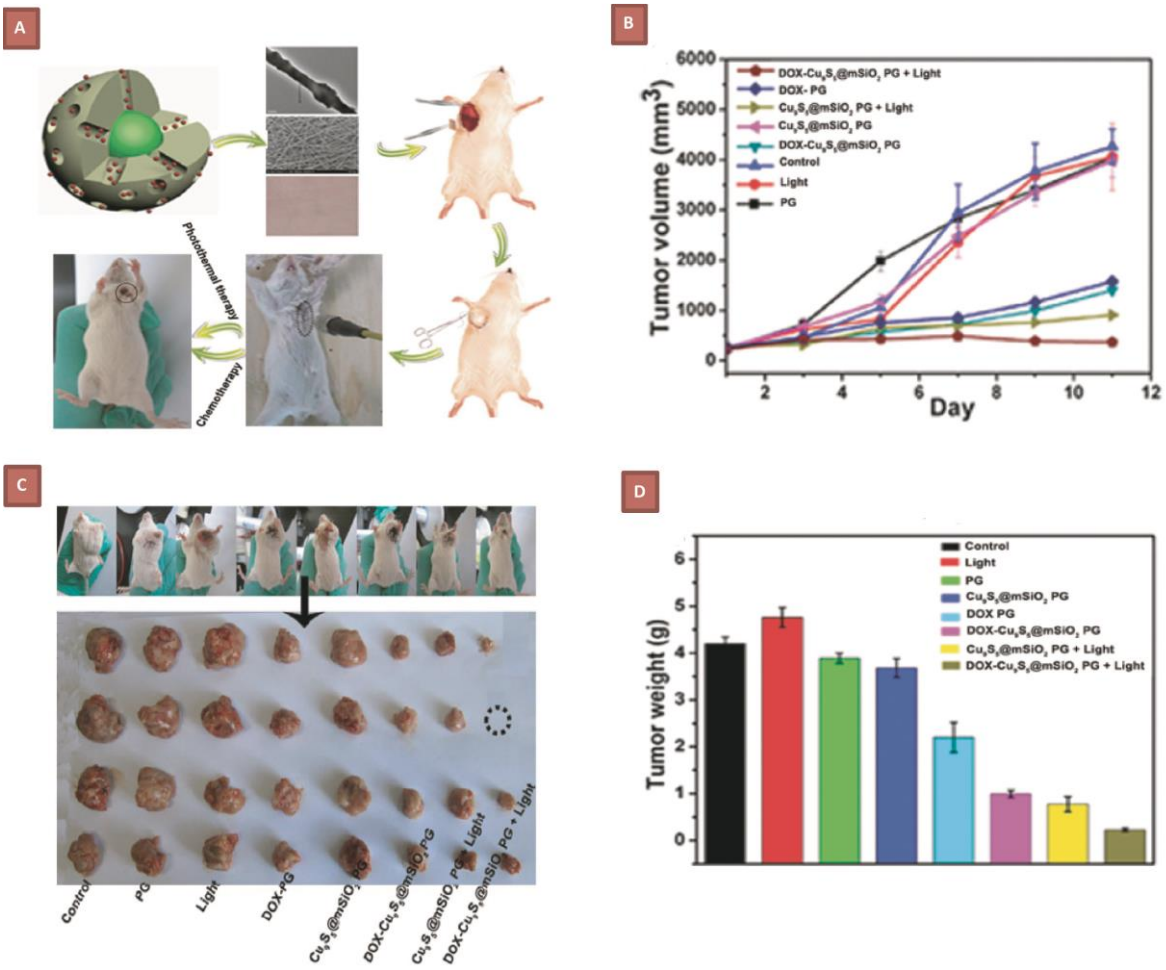

Figure 8. A nanofibrous PCL-based composite for synergistic chemo- and photothermal tumor therapy. A) Schematic showing preparation of composite fibers as well as their subsequent implantation procedure for dual therapy of tumors. B) Tumor volume as a function of time after different treatments. C) Images of mice with tumors and photograph of corresponding excised tumors after 11 days of treatments. D) Mean tumor weights after 11 days of treatments. Reproduced from [151] with permission of The Royal Society of Chemistry.

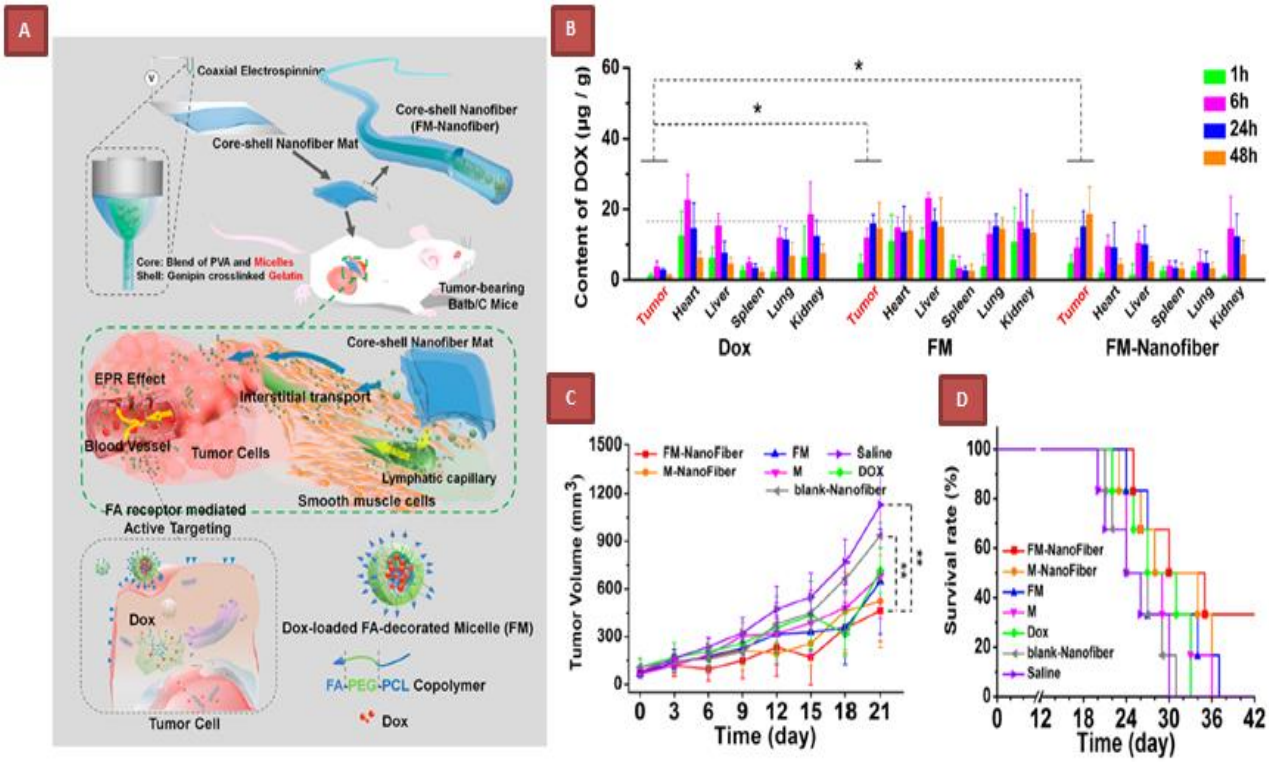

Figure 9. Core-shell micelle-loaded nanofibers for efficient cancer therapy. A) Schematic representation of multi-axial fibers and their corresponding *in vivo* performance. B) Biodistribution (for different time points) in different organs of mice after receiving different treatments. C) Tumor volume and D) survival rate of treated tumor-bearing mice as a function of time. Reprinted with permission from [139], Copyright (2015) American Chemical Society.

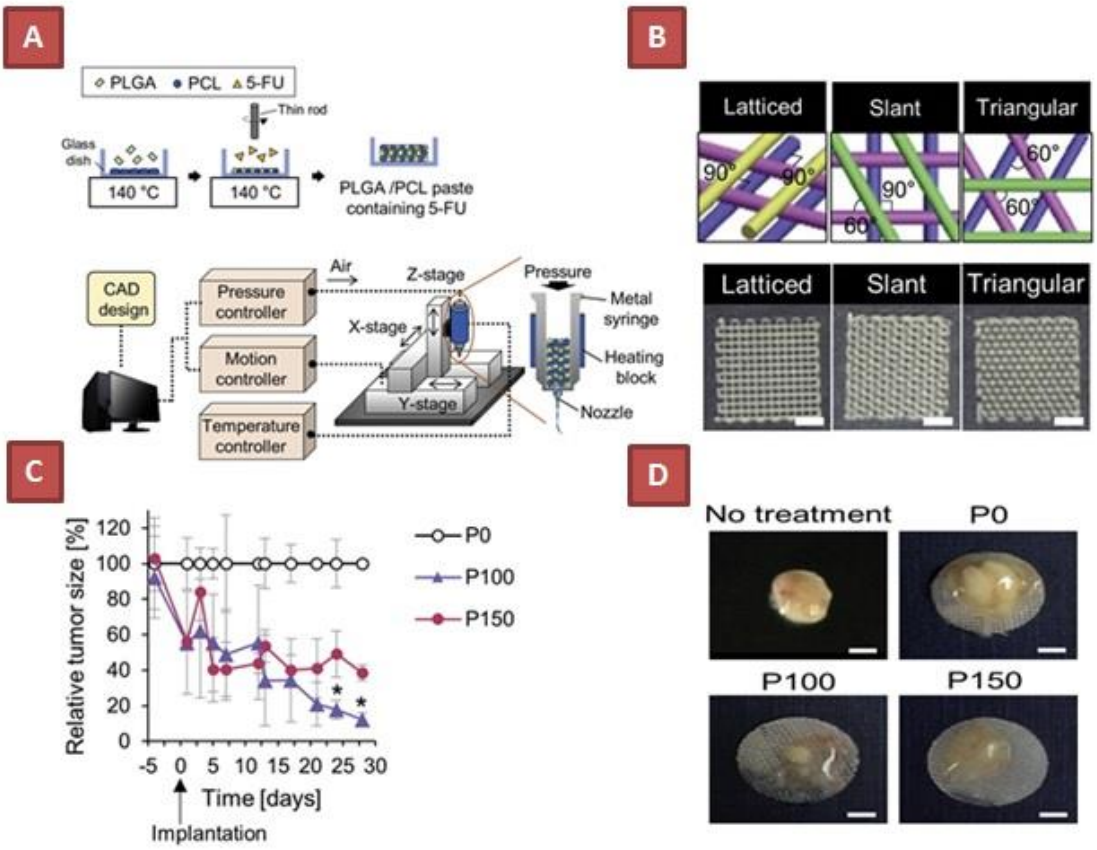

Figure 10. 3D printed patch for local delivery of 5-FU for pancreatic growth suspension. A) Schematic showing sample preparation procedure. B) Schematic and photograph of printed patches with different geometries. C) Relative tumor size as a function of time in mice after implantation of drug loaded patches. D) Photographs of excised tumors and the patches 4 weeks after implantation. Reprinted from [26], Copyright (2016), with permission from Elsevier.

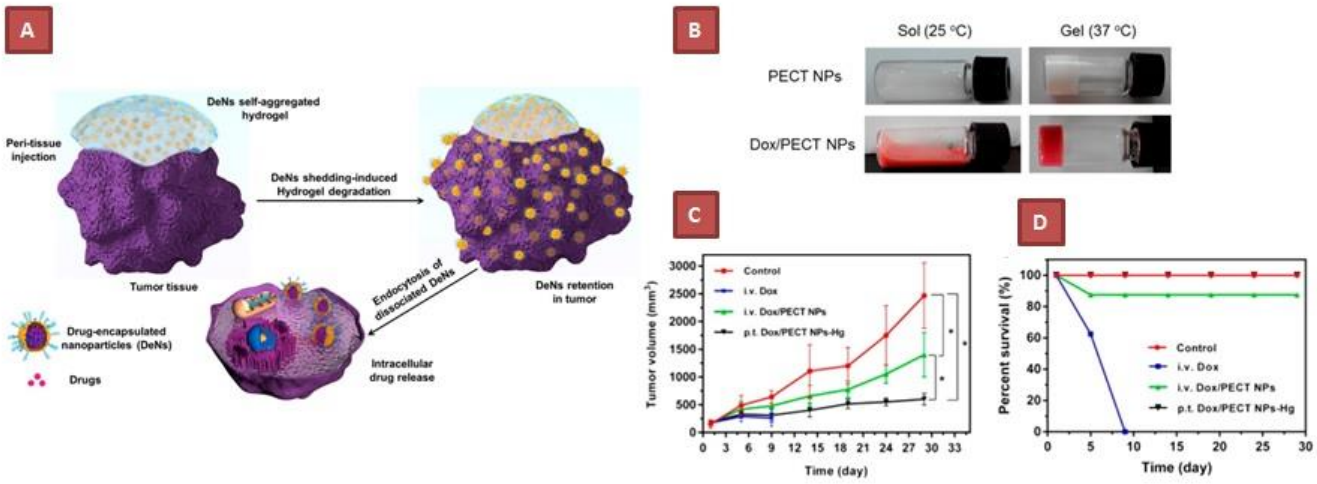

Figure 11. Injectable thermosensitive nanoparticle-assembled hydrogel for peritumoral chemotherapy. A) Schematic showing design concept and *in vivo* mechanism of action of the hydrogels. B) Images of sol-gel transition of hydrogels at 37 °C. C) Tumor volume change and D) percentage of survival, as a function of time, for treated animals. Reprinted with permission from [40], Copyright (2016) American Chemical Society.

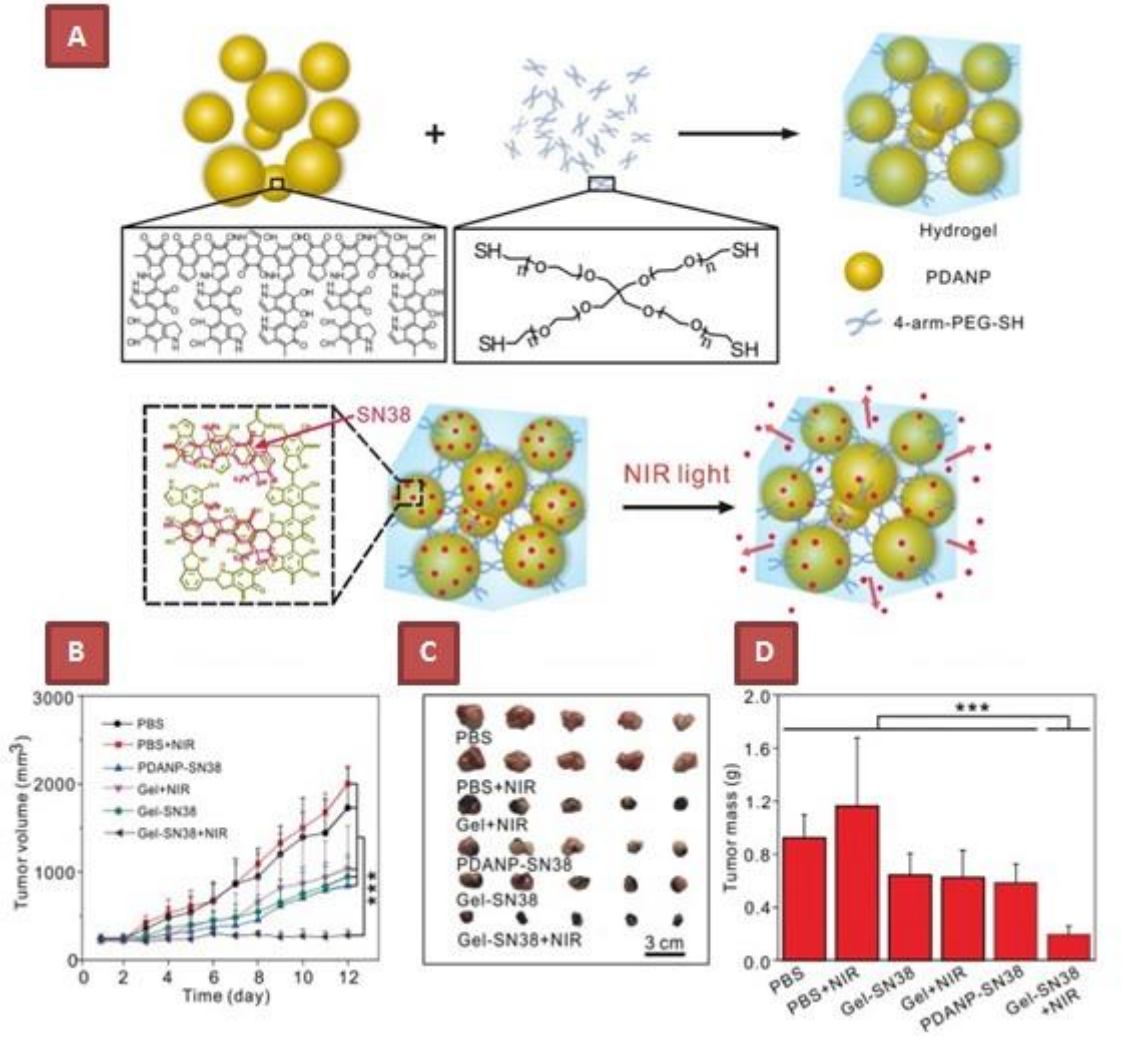

Figure 12. Injectable polydopamine nanoparticle-knotted PEG hydrogel for on demand chemo-photothermal therapy of tumors. A) Schematics showing preparation PDA/PEG hydrogel and subsequent SN38 release mechanism from the hydrogel upon NIR irradiation. B) Tumor volume change plot for different treated groups. C) Photograph of excised tumors and D) their corresponding average weight. Reprinted with permission from [177], Copyright (2017) American Chemical Society.

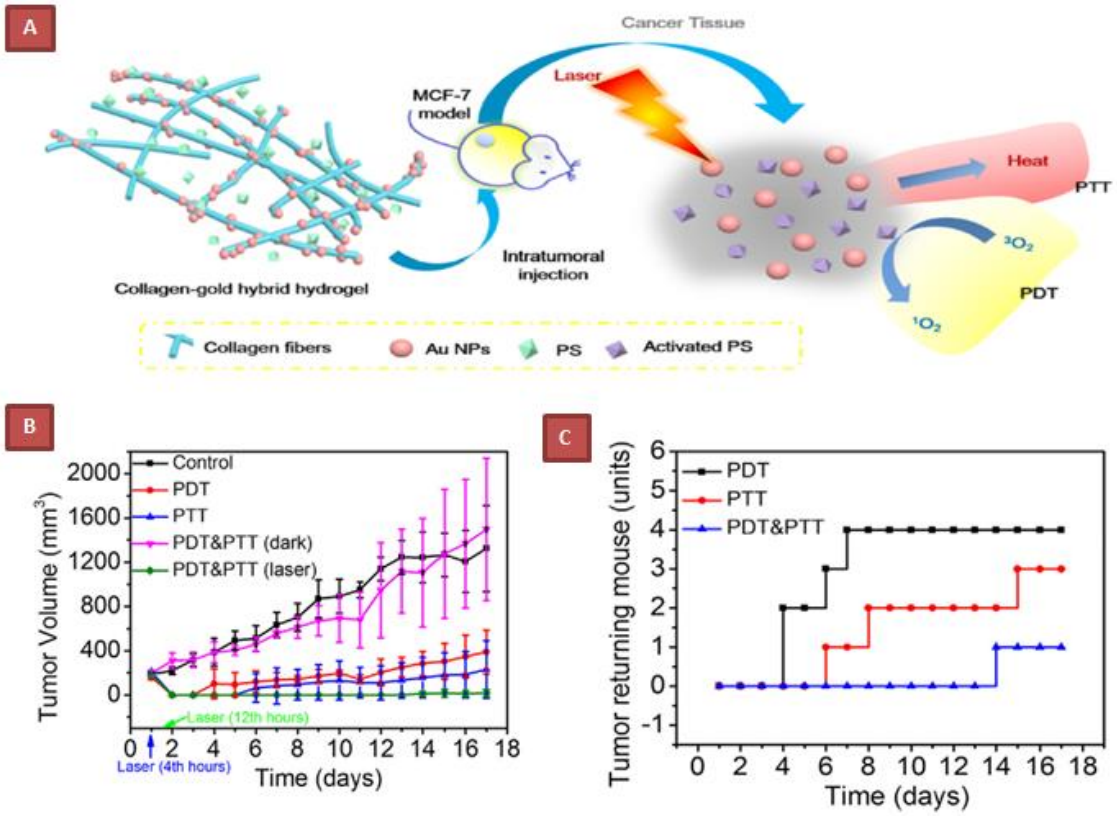

Figure 13. Collagen-based injectable hybrid hydrogel for synergistic photothermal therapy (PTT) and photodynamic therapy (PDT) of breast cancer tumor in mice model. A) Schematic representation of injectable hybrid hydrogel, containing gold nanoparticles (Au NPs) and photosensitizer (PS), and its corresponding *in vivo* anti-tumor mechanism. B) Tumor growth graphs of mice treated with different treatments. C) Tumor recurrence in different groups. Reprinted from [53], Copyright (2017), with permission from Elsevier.

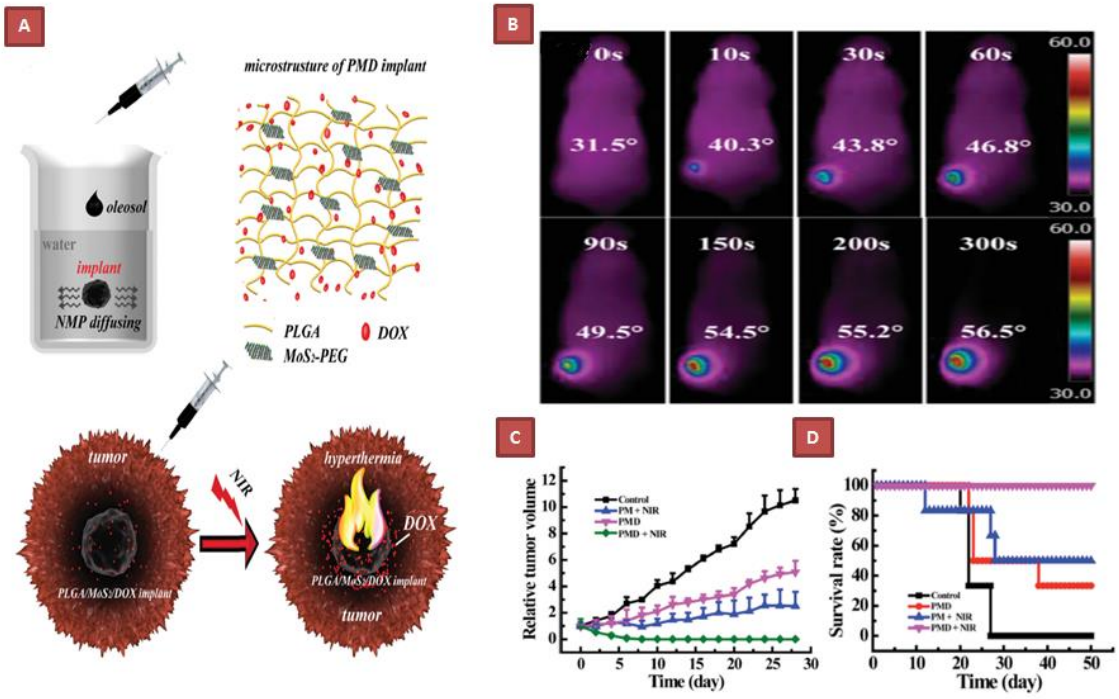

Figure 14. Multifunctional PLGA/MoS_2/DOX (PMD) oleosol as injectable implant for synergistic chemo- and hyperthermia tumor therapy. A) Schematic illustration showing *in vitro* phase transformation of oleosol, oleosol microstructure, and *in vivo* dual mechanism of tumor therapy triggered by NIR irradiation. B) *In vivo* thermal images of PMD implanted mice after continuous NIR irradiation for different durations. C) Tumor volume change in mice with different treatments. D) Survival rate of mice following various treatments. Reprinted from [171], Copyright (2015), with permission from Wiley-VCH.

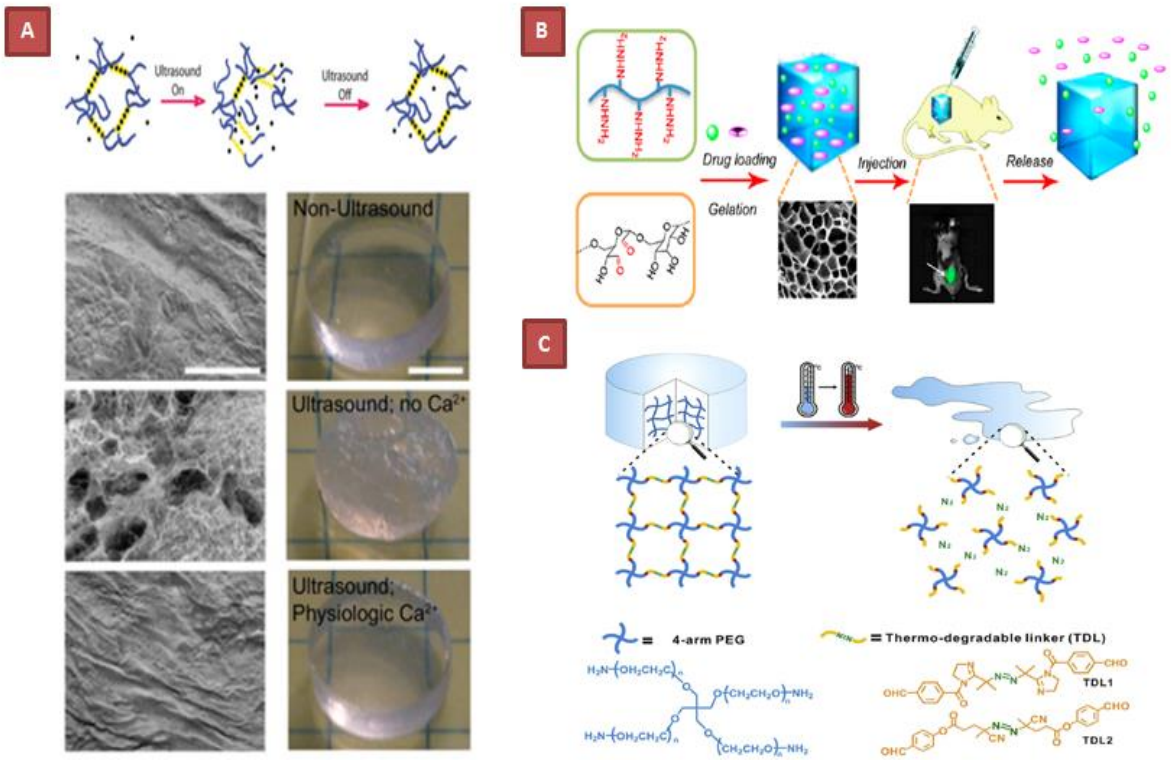

Figure 15. Peculiar characteristics of emerging biopolymers including self-healing, photoluminescence and thermo degradation. A) Ultrasound-trigerred disruption of ionically crosslinked alginate hydrogels and their subsequent self-healing in physiological fluids. Reprinted from [247], Copyright (2014), with permission from National Academy of Sciences. B) Schematic showing preparation of sericin-based hydrogels and their subsequent *in vivo* photoluminescence after implantation. Reprinted from [175], Copyright (2016), with permission from American Chemical Society. C) Schematic illustration of thermal degradation in hydrogels prepared from cross-linking of 4-arm-PEG-NH_2 via thermo-degradable linkers (TDL). Reprinted from [248], Copyright (2017), with permission from Elsevier.

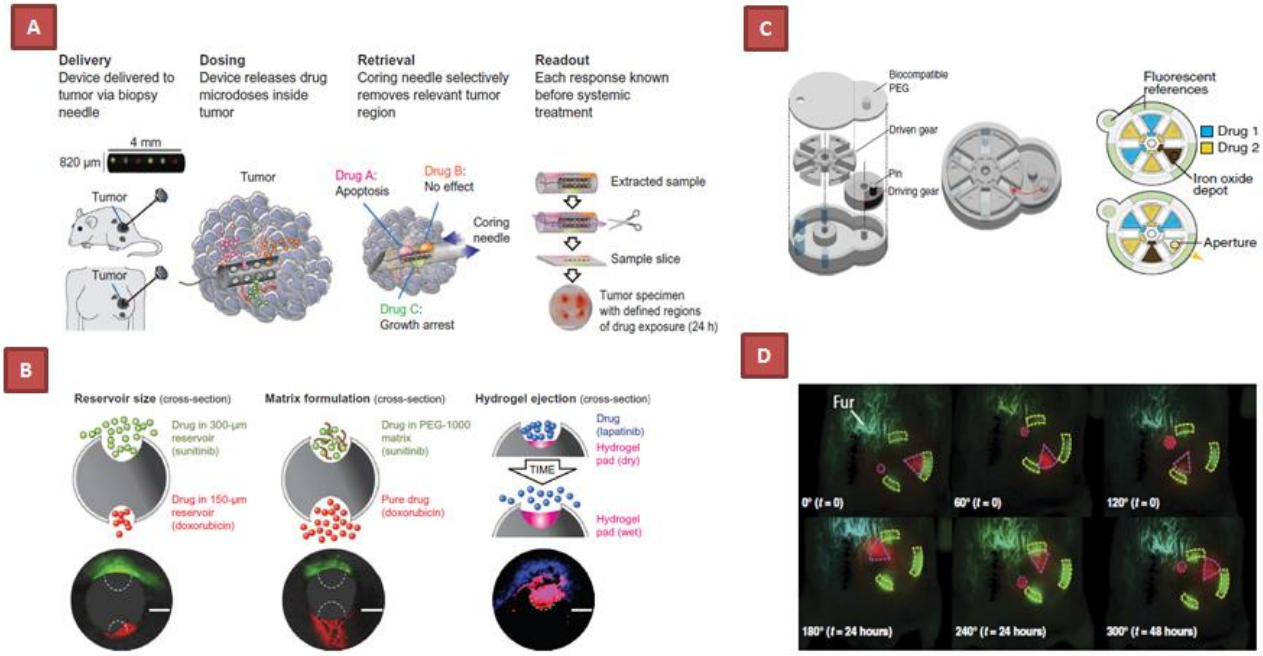

Figure 16. Anti-cancer polymeric micro-devices. A) Schematic Illustrations showing implantation of cylindrical device into the tumor tissue and post processing of the excised tumor section, and, B) Showing three methods used for precise release rate of drugs from each reservoir. From [259], Reprinted with permission from AAAS. C) Schematic representations of geneva drive and single gear implantable MEMS devices made entirely from biocompatible PEGDA, and, D) *In vivo* movement and controlled release of dye from the Geneva drive device. From [268], Reprinted with permission from AAAS.

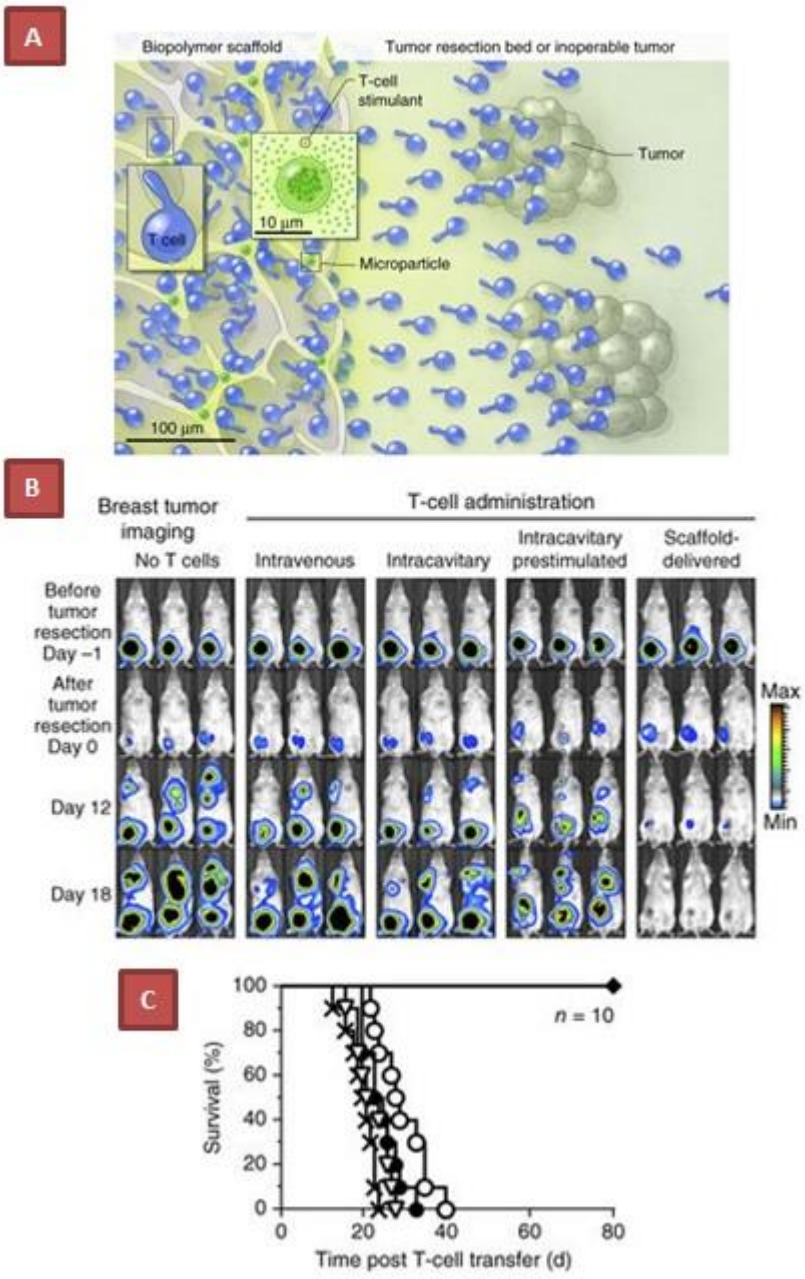

Figure 17. Alginate-based scaffold for delivery of tumor-reactive T cells for treating inoperable or incompletely removed tumors. A) Schematic showing local delivery of T cells to the tumor using the biopolymeric scaffold. B) Bioluminescence imaging of tumors after different treatments. C) Survival curves for mice applied to different treatments. Reprinted by permission from Macmillan Publishers Ltd: Nature Biotechnology [65], Copyright (2015).